Achieving equilibrium as a semi-alluvial channel: anthropogenic, bedrock, and colluvial controls on the White Clay Creek, PA, USA

Sophie Bodek[1*], James E. Pizzuto[1], Kristen E. McCarthy[1†], Raphael A. Affinito[1‡]

[1]Department of Earth Sciences, University of Delaware, Newark, Delaware, USA 19716

Key Points:

- Bankfull Shields stresses are near threshold, but tracers identify abundant immobile clasts derived locally from colluvium and bedrock.
- Channel form is insensitive to sediment supply and channel width reflects cohesive bank processes, rather than bankfull Shields stresses.
- Previous studies identify fluvial equilibrium and anthropogenic and bedrock controls, but *semi-alluvial* is a more applicable term.

*Ramboll US Consulting, Princeton, New Jersey, USA 08540
†Stroud Water Research Center, Avondale, Pennsylvania, USA 19311
‡Department of Geosciences, Pennsylvania State University, University Park, Pennsylvania, USA 16802

Corresponding author: Sophie Bodek, sbodek@udel.edu

Abstract

Based on well-developed hydraulic geometry relations for width and depth, classic studies initially interpreted the Mid-Atlantic White Clay Creek (WCC) as a quasi-equilibrium, alluvial channel. Subsequent studies document the legacy of colonial-age watershed disturbances and urban development, confounding earlier classifications. To investigate this matter, we contribute new data from reach-scale geomorphic mapping, and observations and modeling of bed material transport. WCC's longitudinal profile reflects a history of bedrock incision, while hydraulic geometry equations for width and depth indicate quasi-equilibrium cross-sectional adjustment. Alluvial landforms such as pools and riffles, bars, and actively forming floodplains occur at all 12 study sites, but exposures of bedrock and colluvium are also common. The ratio of bankfull to threshold Shields stress averages 1.41 (range 0.41–2.63), suggesting that WCC is an alluvial, threshold, gravel-bed river. However, a numerical model of WCC bed material transport and grain size, calibrated to bedload tracer data, demonstrates that 22% (range 8–73%) of bed material is composed of immobile, locally sourced cobbles and boulders, while the remaining bed material represents mobile, sand to cobble-sized alluvium; this leads us to classify WCC as a semi-alluvial river. Additional computations suggest that channel morphology is insensitive to bed material supply. Field observations imply that bankfull Shields stresses do not represent channel adjustments to achieve stable banks; rather, width adjustment likely reflects cohesive bank processes. Despite the numerous and contradictory labels applied to WCC (i.e., quasi-equilibrium, Anthropocene, bedrock, semi-alluvial, gravel-bed), each term contributes insight that any single conceptual model would be unable to provide alone.

Plain Language Summary

Geomorphologists rely on conceptual models to categorize fluvial forms and materials. Here we present observations from the White Clay Creek (WCC), a Mid-Atlantic stream, and argue that a multi-faceted conceptual framework is needed to appropriately understand current processes and conditions. Early studies suggested that Mid-Atlantic channels represent an equilibrium state controlled by hydrology, but recently the influence of humans has been emphasized. We add to past observations through geomorphic mapping, monitoring, and modeling of bed sediment movement. The WCC displays typical landforms created through erosion and deposition, such as bars, pools and riffles, and floodplains. Width and depth are well-correlated with water discharge, suggesting hydraulic equilibrium. However, the channel is also bordered by bedrock, gravel derived from adjacent hillslopes, and engineering structures. Furthermore, the WCC longitudnial profile reflects bedrock erosion. Sediment transport monitoring and computations indicate that much of the gravel bed remains immobile when the channel is filled with water, suggesting that the river is not fully capable of sculpting its own channel through erosion and deposition. The WCC reflects many controls, each of which is important: past and ongoing human actions, erosion and deposition of riverine sediment, and occasional exposures of immobile boulders and inerodible bedrock.

1 Introduction

The Shields parameter, most commonly defined by bankfull stage and median grain diameter (D_{50}), has provided a useful means for categorizing the morphology and behavior of river channels (e.g., Church, 2006; Dade & Friend, 1998; Parker, 1979). Coarse-grained rivers often have Shields parameter values slightly in excess of the threshold of motion, which Parker (1978, 1979) and others have interpreted in terms of channel adjustment to transport bed material while maintaining stable banks (Andrews, 1984; Phillips & Jerolmack, 2016, 2019). Somewhat higher Shields stresses reflect active channels subject to rapid lateral shifting and avulsion (Church, 2006). The highest Shields stresses,

often orders of magnitude above thresholds of motion, are typically associated with sand-bed channels whose bed sediment is frequently mobile, even during baseflow conditions (e.g., Church, 2006; Dade & Friend, 1998; K. Dunne & Jerolmack, 2018).

While the Shields parameter has provided a unifying conceptual framework to explain some observations, other studies have documented river channel processes that may not represent adjustments to maintain reach-averaged bankfull Shields stresses. Changes in sediment supply to coarse-grained channels can be modulated by narrowing or widening of zones of active transport or the development of patches of varying sediment mobility (Dietrich et al., 1989; Lisle et al., 2000; Nelson et al., 2009; Seal & Paola, 1995), adjustments that may proceed independently of changes in Shields stress. Sediment supply can also be accommodated by changing the extent and nature of coarse pavement in gravel-bed rivers (Buffington & Montgomery, 1999b; Pfeiffer et al., 2017), or by adjustment of channel roughness (Buffington & Montgomery, 1999a). Recent experimental studies further suggest that channel morphology and sediment transport can be influenced by very small changes in the fraction of the coarsest bed material (MacKenzie & Eaton, 2017; MacKenzie et al., 2018). The concept of partial or marginal transport implies that most grains of a given size at low transport rates may remain immobile; thus mobility of a particular grain size need not imply complete removal of those grains from sloping banks (Andrews, 1994; Wilcock & McArdell, 1997).

In addition to complex interactions between channels and the supply of fluvial sediment, external drivers can also impose important controls on fluvial processes and morphology. Even isolated bedrock exposures and other forms of channel confinement can influence fluvial adjustments in important ways (Fryirs et al., 2016; Meshkova et al., 2012; Turowski et al., 2008; Turowski, 2012). Colluvial and glacial sources of sediment, even if no longer currently active, can strongly impact river channels (e.g., Hassan et al., 2014; Hauer & Pulg, 2018; Polvi, 2021; Snyder et al., 2009), leading Ashmore and Church (2000) to define *semi-alluvial* channels as those whose adjustment is limited by relatively immobile sediment supplied by non-fluvial sources. The growing awareness of anthropogenic controls on stream channels has lead to the recent concept of *Anthropocene streams*, rivers where humans have substantially influenced channel morphology (Jacobson & Coleman, 1986; James, 2019; Merritts et al., 2011, 2013; Walter & Merritts, 2008).

Here we present observations of a watershed where these diverse controls are manifested. An initial interpretation based on Shields parameter values and casual surveys suggests the White Clay Creek is a near-threshold, alluvial, gravel-bed river, whose morphology is adjusted to achieve stable banks. However, additional observations document the occurrence of relatively immobile cobbles and boulders, likely supplied by erosion of colluvium and weathered bedrock, and a channel profile that reflects long-term bedrock incision. Deposits arising from past anthropogenic watershed disturbances are abundant and well-documented; however, we also present evidence of ongoing adjustment to the current hydraulic regime. Categorizing fluvial processes in this setting requires identifying the origin of fluvial sediments, their history, and careful observations of ongoing processes. Channels in our study area embody many different paradigms of fluvial geomorphology, but we will argue that they most clearly reflect the emerging concept of the semi-alluvial river by exhibiting salient features of alluvial gravel-bed channels, while also being subject to important non-fluvial controls: immobile colluvial cobbles and boulders, frequent bedrock exposures, and localized landforms forced by human disturbances.

2 Study Area

The White Clay Creek watershed covers 279.2 km^2 in southeastern Pennsylvania and northern Delaware (Figure 1a). Land uses include developed areas (38%), agriculture (32%), forest (28%), and wetlands (2%) (Kauffman & Belden, 2010). The region has a modified humid continental climate with moderately cold winters and warm, hu-

mid summers. Water discharge and other data are collected at four U.S. Geological Survey (USGS) stream gages, and also at the Stroud Water Research Center (Figure 1a). Data from the stream gage near Strickersville, PA (USGS gaging station #01478245) are particularly important for this study.

The White Clay Creek watershed encompasses two physiographic provinces. The northern portion of the watershed lies within the Piedmont Physiographic Province (Fischer et al., 2004; Renner, 1927), which is underlain by deeply weathered late Proterozoic and early Paleozoic metamorphic rocks (Christopher & Woodruff, 1982; Schenck et al., 2000). Near Newark, DE, the White Clay Creek encounters the Fall Zone, which represents the boundary between the Piedmont Province to the north and the Coastal Plain Physiographic Province to the south. Here the White Clay Creek abruptly turns to the east and encounters Cenozoic sedimentary rocks (Plank et al., 2000; Ramsey, 2005). Immediately north of Newark, DE, the valley of the White Clay Creek is incised through the Old College Formation (Figure 1b, 1c), a middle Pleistocene (770-126 ka) alluvial fan deposited by an ancestral White Clay Creek (Ramsey, 2005).

Fluvial geomorphologists have long recognized the Fall Zone as an important regional control on fluvial morphology in the Mid-Atlantic region. Northwest of the Fall Zone, rivers reflect the tectonic and erosional history of the Piedmont Province, which Hack (1982) interpreted as a balance between uplift and erosion, creating a landscape characterized by steady-state topography. Analyses of ^{10}Be and its geologic context support this hypothesis, and indicate rates of uplift and denudation of approximately 4 m/Ma in the Virginia Piedmont (Pavich et al., 1985). To the south and east of the Fall Zone, the landscape reflects Cenozoic downwarping of the Coastal Plain (Pazzaglia, 1993). During the Pleistocene, streams near the Fall Zone were influenced by meltwater from downwasting Pleistocene ice sheets (Reusser et al., 2004), crustal movements related to the migration of the glacial forebulge (Pico et al., 2019), and an influx of periglacial colluvium that at least partially filled river valleys (Costa & Cleaves, 1984; Del Vecchio et al., 2018; Walter & Merritts, 2008).

3 Background and Hypotheses

3.1 Previous research in the study area and region

Wolman (1955) presented hydraulic geometry relations for the Brandywine Creek watershed, which is located adjacent to and northeast of the White Clay Creek. He described typical features of alluvial channels such as pools, riffles, and floodplains, but also noted bedrock exposures and knickpoints along the stream's longitudinal profile. In assessing the importance of bedrock, he noted the presence of fluvially-constructed floodplains consisting of fine sediments alongside a bedrock outcrop, indicating the ability of the Brandywine Creek to adjust its channel and maintain *quasi-equilibrium* (Wolman, 1955).

Subsequently, fluvial geomorphologists documented past anthropogenic activities that continue to influence contemporary stream processes. Accelerated upland erosion led to widespread valley alluviation following European colonization, a process that was enhanced by tens of thousands of mill dams (Walter & Merritts, 2008). Merritts et al. (2011) proposed that Mid-Atlantic channels should be considered *Anthropocene streams* whose nature and history are largely a result of human actions. Other studies, however, have documented contemporary floodplain formation by lateral channel migration (Donovan et al., 2015; Jacobson & Coleman, 1986) and widespread sedimentation across Piedmont river valleys by contemporary overbank flows (Hupp et al., 2013; Noe et al., 2020; Pizzuto et al., 2016; Schenk et al., 2013), suggesting that these "natural" processes are still ongoing despite the region's history of profound anthropogenic disturbance.

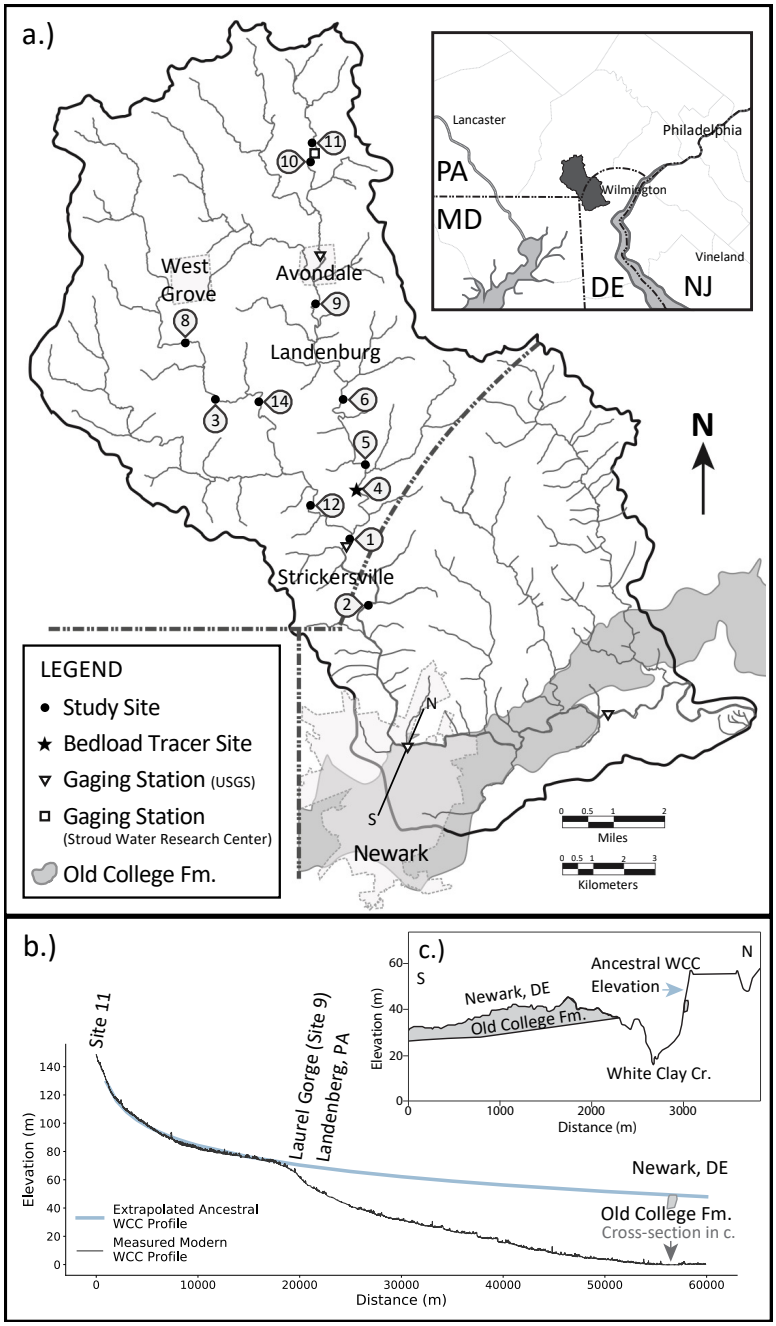

Figure 1. Location, setting, and longitudinal profile of the White Clay Creek. (a) Map of the White Clay Creek watershed showing the locations of 12 study sites, including the bedload tracer study site established at Site 4, and the locations of stream gaging stations. The USGS stream gage near Strickerville, PA is just downstream of Site 1. Also indicated is the extent of the Old College Formation, a middle Pleistocene alluvial fan deposited by an ancestral White Clay Creek, and the line of cross-section of Figure 1c. Inset indicates the regional location of the White Clay Creek watershed. (b) Longitudinal profile of the East Branch of the White Clay Creek from Site 11 to Newark, DE. The profile of the ancestral White Clay Creek, shown in light blue, runs through the Old College Formation. (c) Cross-section of the White Clay Creek's valley near Newark, DE, highlighting exposures of the Old College Formation on both sides of the valley.

Meanwhile, other studies document controls on bank erosion and width adjustment in Mid-Atlantic Piedmont streams. Rates of bank retreat are generally low, typically averaging a few decimeters or less per year (Allmendinger et al., 2005; Rhoades et al., 2009; Pizzuto & Meckelnburg, 1989). Eroding bank sediments are generally cohesive; Pizzuto and Meckelnburg (1989) observe that at certain locations at the nearby Brandywine Creek, the entirety of the bank height consists of cohesive sediments, suggesting that bank erosion is decoupled from mobility of the sand and gravel comprising the streambed. Bank erosion is related to hydraulic forcing (Pizzuto & Meckelnburg, 1989), but loosening of bank soils by freeze-thaw is a necessary precursor for significant erosion (Inamdar et al., 2018; Merritts et al., 2013; Pizzuto, 2009; Wolman, 1959). Bank erosion mostly occurs through very small, frequent (monthly) bank failures (Pizzuto et al., 2010).

Bank erosion rates are reduced where banks are reinforced by roots of mature trees (Allmendinger et al., 2005; Pizzuto & Meckelnburg, 1989); however, forested channels of Mid-Atlantic Piedmont streams are paradoxically wider than channels with grassy riparian zones (Allmendinger et al., 2005; Hession et al., 2003; Sweeney et al., 2004). This observation has also been noted by Trimble (1997) in Wisconsin, USA, and Davies-Colley (1997) in New Zealand. Allmendinger et al. (2005) explain this phenomenon through a bar-push mechanism, where width adjustment is not directly controlled by bank stability and erosion thresholds, but rather reflects a balance between inner bank depositional processes and outer bank erosional processes associated with active channel migration. They propose a model whereby equilibrium width is related to the ratio E/α, where E is a dimensionless bank erodibility coefficient that directly scales with erosion rate (higher E implies faster erosion), and α is a parameter that reflects the effectiveness of vegetation in trapping sediment on the insides of migrating bends. The data of Allmendinger et al. (2005) indicate that E is higher in non-forested channels by a factor of 3 compared to forested channels, which by itself would suggest wide grassy channels and narrow forested channels (opposite to what is observed). However, dense grasses growing on depositional banks lead to values of α along grassy channels that exceed those of forested channels by a factor of 5, as dense grasses are shaded out in forest reaches, reducing deposition rates along the inside banks of forested channels. Essentially, very high values of α in grassy channels offset relatively high values of E; thus, the ratio of E/α is lower in grassy channels than in forested channels, providing a mechanistic explanation of why forested channels are wider than grassy channels despite the increased erosion resistance imparted by trees in forested channels.

3.2 Hypotheses

Our study was designed to test specific hypotheses derived from previous research and our own preliminary field observations. These hypotheses are summarized graphically in a conceptual diagram (Figure 2). The White Clay Creek appears to be locally confined both laterally and vertically by bedrock (Wolman, 1955) and colluvium (Walter & Merritts, 2008), and also bordered by valley fill deposits of diverse origin primarily consisting of mixtures of sand, silt, and clay. Sediments supplied locally to the channel appear to consist of colluvium and weathered bedrock ranging in size from clay to boulders, and somewhat finer sediments supplied by eroding valley fill deposits. Our initial field observations also suggest that sand and gravel are supplied by fluvial transport from upstream; this fluvially transported material is referred to as *throughput load* (Li et al., 1976). Sediments on the streambed range from sand to boulders, reflecting both colluvial and fluvial sources. We hypothesize that isolated bars are created by, and store frequently transported bedload consisting of sand and pebbles. Furthermore, we hypothesize that exposed bedrock and colluvially-sourced cobbles and boulders on the streambed are evidence of low sediment supply and non-fluvial controls on channel morphology, while eroding streambanks imply the potential for cross-sectional adjustments from fluvial processes.

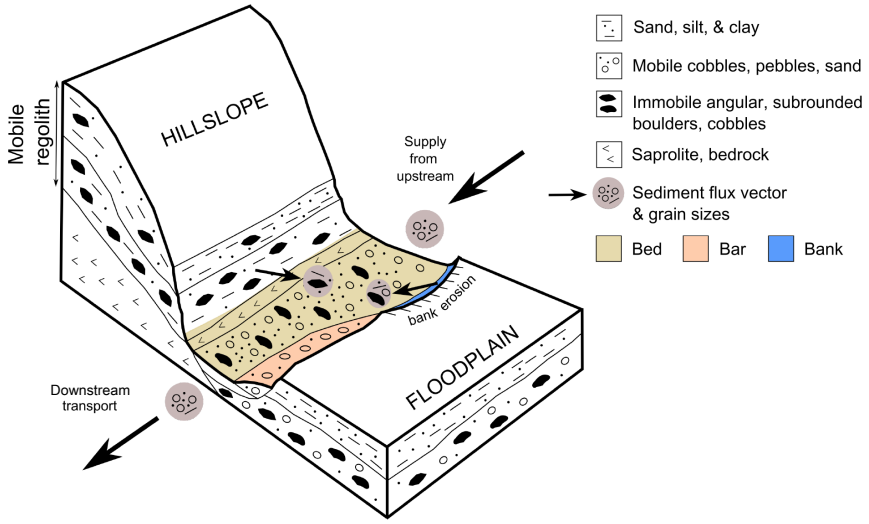

Figure 2. Preliminary conceptual model of bed material supply and flux in the White Clay Creek. Immobile cobbles and boulders are supplied locally through bank erosion and channel incision, while the fluvial supply from upstream consists of sand and pebbles stored in bars. The streambed is anchored by cobbles and boulders that are immobile at bankfull stage, but contains a sparse covering of throughput load consisting of sand and pebbles primarily supplied from upstream (but augmented by locally eroding banks).

4 Methods

We designed a field program to evaluate the conceptual model summarized in Figure 2. A longitudinal profile of the White Clay Creek watershed is used to assess relationships between fluvial processes and the underlying bedrock. Studies of reach-scale stream morphology and grain size over a range of stream orders provide estimates of bankfull Shields stresses across the watershed. Geomorphic mapping, stratigraphic analyses, and measurements of bank erosion rates provide additional data. To more precisely assess the mobility of sediments of varying sizes, radiotracers were installed in bed sediments at one site and monitored over four significant flow events. These data were used to calibrate an equation for the motion of individual bedload grain size fractions. Once calibrated, this equation was used to assess the mobility of different grain sizes at our field sites at bankfull stage, and to better understand the relationship between bed mobility and bankfull Shields parameter values. The calibrated bedload transport model was also used to determine the sensitivity of the White Clay Creek channel to changes in bed material supply.

4.1 Current and ancestral longitudinal profile

Watershed-scale geologic controls on channel morphology were documented by creating a longitudinal profile of the current White Clay Creek. Channel centerlines were first hand-drawn in an ArcGIS environment from high-resolution aerial imagery. Centerlines were extended upstream until the channel could no longer be clearly identified. Elevations along the centerline were then extracted from a Digital Elevation Model created from aerial LiDAR survey data.

The current longitudinal profile of the White Clay Creek displays two concave-upwards segments that meet at a prominent knickpoint in Laurel Gorge just upstream of Lan-

denburg, PA (Figure 1b, 1c). We hypothesize that the uppermost concave-upwards segment corresponds to the remnants of an ancestral White Clay Creek, whose profile represented an approximate balance between long-term fluvial incision into bedrock and ongoing uplift (e.g., Hack, 1982; Pavich et al., 1985). To estimate the form of this ancestral profile, we considered the equation for time-dependent bedrock fluvial incision (Whipple & Tucker, 1999):

$$\frac{\partial z}{\partial t} = U - Bx^M \left(-\frac{\partial z}{\partial x}\right)^N \tag{1}$$

where z is the elevation of the channel profile at a distance x from the divide, t is time, U is the uplift rate, and B, M, and N are coefficients. If the coordinates of two points along a profile are known, and if the incision rate and uplift rates are equal everywhere along the profile, the following solution can be obtained:

$$z = (z_1 - z_2)\frac{(x_2^{1-Q} - x^{1-Q})}{(x_2^{1-Q} - x_1^{1-Q})} + z_2 \tag{2}$$

where the subscripts 1 and 2 denote x and z values of two locations along the ancestral steady-state longitudinal profile, and Q is the concavity parameter M/N. We used equation (2) to determine the form of the ancestral White Clay Creek's profile by selecting two known points from the uppermost concave-upwards segment of the White Clay Creek's current profile, and varying the value of Q until a satisfactory fit was obtained to the preserved uppermost concave-upwards segment.

4.2 Documenting reach-scale fluvial morphology

Twelve sites were selected to document reach-scale characteristics of the White Clay Creek (Figure 1a, Table 1). All of the sites are within the Piedmont Physiographic Province and all except one are located in Pennsylvania; the lone site in Delaware is about 1 km downstream of the Pennsylvania border. Study reaches varied from 157 to 811 m in length; riparian zones were both forested and in pasture (Table 1). Five sites are influenced by engineering structures, including abandoned railroads, and at one site, historic rip-rap along one of the banks. Breached or extant colonial mill dams are located within 0.4–2.1 km either upstream or downstream of several study sites (Table 1).

Survey data document the morphology and bed and bar grain size distributions at the 12 sites. One cross-section was surveyed at each site, except Site 4 (the location of the bedload tracer study), where three cross-sections were surveyed. Sections were located at relatively straight reaches or at inflection points between bends. Bankfull width and depth were defined by the inflection points between steeply sloping banks and the adjacent valley flat. Where bankfull stage could be defined by inflection points at each bank, the lower of the two inflection points was selected as the bankfull stage, similar to the procedure described by T. Dunne and Leopold (1978) for a location at the Stroud Water Research Center near our Site 11 (McCarthy, 2018).

Longitudinal profiles document slopes of the water surface and streambed along the channel centerline. The grain size distribution of the bed and bar material at each study site was determined using the Wolman (1954) method. Samples of the streambed were selected at equally spaced intervals along the center of the channel through a reach encompassing a minimum of 3 pool-riffle sequences. Clasts on bars were selected by stepping randomly across bar surfaces. Samples consisted of at least 100 clasts, resulting in a minimum error of 20% for individual grain size percentiles (Rice & Church, 1996).

Geomorphic maps document each site's geomorphic setting. Mapped features included exposures of bedrock and colluvium, large boulders on the streambed, anthropogenic structures (e.g., old railroad grades, rip rap, etc.), large wood, type of riparian

vegetation, pools and riffles, locations of tributaries, side channels, eroding banks, and various types of bars.

The stratigraphic setting was documented through measurements and observations of deposits exposed in eroding banks, and by creating a geologic cross-section at Site 1. Deposits were classified visually and interpreted in the context of previous studies of valley-fill sediments of the Mid-Atlantic region (Jacobson & Coleman, 1986; Walter & Merritts, 2008). At Site 1, sediments were sampled using a bucket auger along a surveyed topographic cross-section.

Decadal average rates of eroding bank retreat were measured at each site. Erosion rates were measured using a combination of repeat historical aerial imagery (Rhoades et al., 2009) and dendrochronology (Stotts et al., 2014). Detailed discussion of methods and results are presented by McCarthy (2018).

4.3 Bedload tracer study

Bedload tracer particles were installed during the summer of 2019 at a 100 m reach at Site 4, which is located approximately 2.8 km upstream of the Strickersville gaging station (Figure 1a). Tracer particles consisted of 32 mm HDX (half duplex) RFID (radio frequency identification) tags manufactured by Oregon RFID. The tags were placed at random locations throughout the reach and were attached to a wide range of sediment sizes. The first RFID tags were installed in June through early July 2019 and the grain size distribution of the tagged clasts mirrored the grain size distribution of the bed. Additional clasts were tagged in late July 2019 and in October 2019, resulting in a total of 56 tagged clasts ranging in size from 10 mm to 1,440 mm.

The tracers were installed in situ on the streambed by drilling holes into clasts that were exposed above the surface of the water at low flow. The RFID tags were placed in the holes and sealed in place with a waterproof epoxy. Tags were installed in situ wherever possible in order to prevent our actions from disturbing the bed and increasing the likelihood of transport. In order to tag clasts that were underwater, the waterproof epoxy was used as a glue to attach a tag to the surface of each clast. If clasts were sufficiently small (10–50mm), the tag could not be affixed without disturbing the bed. These small clasts were removed from the streambed in order to attach the RFID tag.

After installation, tagged particles were surveyed at regular intervals. Surveys occurred weekly during July 2019 with subsequent surveys occurring monthly from August 2019 to January 2020. A total of nine surveys were completed over the course of the study (not including the initial survey that first established clast location). For all surveys, the RFID tags were located using an antenna reader manufactured by Oregon RFID with a 0.5 m detection radius. Once a tagged clast was found, its location was recorded using an electronic total station located above a benchmark on a gravel bar. Since the detection radius of the RFID reader antenna is 0.5 m (Phillips & Jerolmack, 2014), the detection threshold was set to the same value, with all tracer motion below 0.5 m considered as error and set to zero. Tracer recovery ranged from 100–66%. The recovery rate of the final survey, which occurred in January 2020, was unusually low (66%) due to the occurrence of a flow event that nearly reached bankfull stage. It is likely that several tagged clasts were transported out of the study reach, or onto the bar or banks where they were not detected.

The water level in the reach was surveyed for two significant flow events on 27 October 2019 and 25 January 2020. Within 3 days after each event, the high water marks on both sides of the channel were flagged based on observations of disturbed leaves, flattened vegetation, or debris left along the bank. Later, the flagged high water marks were surveyed using an electronic total station or automatic level. The location of each tagged clast was also recorded during these surveys. The difference in height between the tracer

Table 1. Location and Geomorphic Setting of 12 Study Sites

Site no.	Location	Stream order	Reach length	Sinuosity	Fraction[a] exposed bedrock and colluvium	Fraction[a] with at least 1 eroding bank	Riparian vegetation[b] of outer bank	Side channels or mid-channel bars present	Fraction[a] influenced by anthropogenic structures	Type of structure[c]	Distance, direction[d] to nearest mill dam[e]
	[°N, °W]	[–]	[m]	[–]	[–]	[–]	[–]	[–]	[–]	[–]	[km]
1	39°44'55.16", 75°46'11.67"	4	157	1.04	0	0.81	Forest	No	0.17	Bridge, RR	1.3, ds, B
2	39°43'44.70", 75°45'40.16"	4	198	1.74	0	1	Pasture	Yes	0	none	1, us, E
3	39°47'11.44", 75°49'8.24"	2	316	1.22	0.12	0.66	Pasture	Yes	0	none	none
4	39°45'47.48, 75°45'59.61"	3	170	1.27	0.34	0.48	Forest	Yes	0.18	RR	2.1, us, E
5	39°46'6.56", 75°45'46.58"	3	184	1.36	0.25	0.49	Pasture	No	0	none	1.2, us, E
6	39°47'5.57", 75°46'27.45"	3	811	1.09	0.79	0.25	Forest	No	0.36	RR, BCMD	0.5, ds, B
8	39°48'12.96", 75°49'47.63"	2	326	1.05	0.09	0.49	Pasture	Yes	0.08	ECMD	0.4, ds, E
9	39°48'47.07", 75°47'4.64"	3	214	1.79	0	0.74	Forest	No	0	none	1.8, ds, B
10	39°51'21.32", 75°47'1.28"	2	678	1.43	0.06	0.85	Pasture	No	0	none	none
11	39°51'40.61", 75°47'2.51"	2	610	1.12	0.30	0.76	Forest	No	0	none	none
12	39°45'19.89", 75°47'8.33"	3	504	1.36	0.59	0.31	Forest	Yes	0.17	riprap	1.3, ds, E
14	39°47'9.31", 75°48'10.98"	2	514	1.02	0.51	0.86	Forest	No	0	none	none

[a]Fractions are by reach length. [b]Forested—tree density > 0.3 trees/m^2, see McCarthy (2018) for details. [c]RR—railroad, BCMD—breached colonial mill dam, EMCD—extant colonial mill dam, riprap—historic bank stabilization by boulders. [d]ds—downstream, us—upstream. [e]B—breached, E—extant.

manuscript submitted to *JGR: Earth Surface*

and nearest high water mark was utilized to determine the depth of water above that clast.

4.4 Calibrating a bedload transport model

To assess bedload transport at the various study reaches, we use the sediment transport model developed by Wilcock and Crowe (2003) that determines the transport rate for mixed sediment sizes, including sand. This model is chosen due to the utilization of the full grain size distribution of the bed surface and its wide applicability.

Bedload tracer data are used to calibrate the sediment transport model for conditions at the White Clay Creek. Similar to many other sediment transport equations, the Wilcock and Crowe (2003) sediment transport model requires a reference shear stress (τ_{*ri} or τ_{ri}) (e.g., Parker, 1990; Parker & Klingeman, 1982; Parker et al., 1982; Wilcock, 2001), defined as the Shields stress (τ_*) or shear stress (τ) at which a dimensionless transport parameter is equal to a reference value (Parker et al., 1982). This reference value ($W_{*r} = 0.002$) represents a threshold of motion, where sediment sizes with a dimensionless transport parameter less than the reference value ($W_{*i} < 0.002$) are considered immobile (Parker et al., 1982).

While the value of the reference shear stress can be determined using a variety of approaches (e.g., Parker et al., 1982; Segura & Pitlick, 2015; Wilcock & Crowe, 2003), the data collected in this study are poorly suited to previous methods. Here we define the reference shear stress (τ_{ri}) as the stress that is required to transport a particular particle by a distance equal to its diameter.

The shear stress generated by each flow event was determined using the depth-slope product: the flow depth for each event was determined by correlating the measured depth in the study reach (determined by the high water mark surveys and cross-sectional surveys) to the gage height at the downstream Strickersville gage; the slope was held constant and equal to the bed slope. It is assumed that the highest flow event prior to each survey was responsible for mobilizing the bedload tracers. The distance traveled by each tracer was normalized by grain size; we could then relate normalized distance traveled to shear stress over the recorded flow events for each grain size category. The range of reference shear stresses was defined as the span of values between a measurement of insignificant motion (a movement of less than one grain diameter) and a measurement of significant motion (greater than one grain diameter); the average of this range is considered the reference shear stress for a given grain size. In certain cases when significant motion was observed during even the lowest flow event, the shear stress required to transport a tracer by a distance of one grain diameter was founding using a linear regression model; a detailed discussion of methods is presented by Bodek (2020).

Thus, a range of reference shear stresses for each grain size category (τ_{ri}) could be determined. A relationship between grain size and average reference shear stress could then be ascertained for all grain sizes, even those too small to tag or too large to be mobilized by conditions observed during the study period. Thus, two important parameters were found—the reference shear stress for the mean grain size (τ_{rm}) and the hiding function exponent (b), which are utilized in the following hiding function:

$$\tau_{ri} = \tau_{rm} \left(\frac{D_i}{D_m} \right)^b \tag{3}$$

where τ_{rm} is the reference shear stress for the geometric mean grain size (D_m), τ_{ri} is the reference shear stress for a given grain size (D_i), and b is the hiding function exponent. The reference shear stress, τ_{ri}, and b have been observed to vary in different environments (e.g., Andrews & Parker, 1987; Kuhnle, 1993; Parker et al., 1982; Wilcock, 1993), necessitating field-based observations when determining these values.

Due to the range of reference shear stresses found for each grain size category, a 5% and 95% confidence interval was used to find the upper and lower range of the reference shear stress and the hiding function exponent. The hiding function, which increases the mobility of large grain sizes that have a greater surface area exposed to the flow and reduces the mobility of smaller grain sizes that tend to be hidden amongst larger clasts, has the ability to significantly alter the outcome of the sediment transport model. We use the upper and lower limit of the hiding function exponent to assess uncertainty in computations that rely on the Wilcock and Crowe (2003) sediment transport equation.

4.5 Predicting the mobility of bed and bar sediments at bankfull stage

As the calibrated Wilcock and Crowe (2003) sediment transport model determines transport rate for various grain sizes, it can be used to evaluate the mobility of sediments at different reaches in the White Clay Creek watershed. By applying the sediment transport model to the bed and bar grain size distribution at each study site, the largest grain size predicted to be mobile at bankfull conditions is determined based on the dimensionless transport parameter W_{*i}. For these computations, the bankfull depth and reach-averaged bed slope were used to determine shear stresses on both the bar and the streambed. We did not assess differences in shear stress associated with complex bar topography at each site. Grain sizes are no longer considered mobile when $W_{*i} < 0.002$ (Parker et al., 1982). These methods are used to test two of our preliminary hypotheses: (1) that a significant fraction of the bed is immobile at bankfull stage, and (2) that sediments comprising the bar represent stored alluvium that is mobile at bankfull stage.

4.6 Model computations to assess sensitivity to changes in bed material supply

A numerical model was developed to predict bed material grain size distribution and bed elevation of a gravel-bed reach based on channel geometry and sediment supply. The model is informed by the study reaches in the White Clay Creek watershed with initial and boundary conditions based on field observations. We use the model to perform numerical experiments to determine the extent to which our sites are under-supplied by alluvial bed material transported from upstream. Experiments are performed by increasing the flux of throughput load (assumed to have the same grain size distribution as the bar sediments of the White Clay Creek) until the bed has aggraded to create a fully developed active layer with a mean grain size similar to that of the sediment supply, which we interpret as representing a transition from the existing semi-alluvial channel to an alluvial channel whose bed fully reflects sediment supplied from upstream. We interpret the amount of sediment required to affect this transition as one metric for quantifying the extent to which our sites are semi-alluvial rather than fully alluvial channels.

4.6.1 Conceptual framework and design of numerical experiments

Consistent with our conceptual model (Figure 2), our approach is based on the idea that the bed of the White Clay Creek consists of partially mobile material (i.e., throughput load) overlying relatively immobile colluvium and bedrock. Furthermore, we envision that the thickness of stored sediment is less than the active layer accessible to the flow for bed material transport (Parker, 1991, 2008), and that the bed as a whole does not have a coherent coarse surface layer or pavement. This conceptualization of an undersupplied, partially armored stream bed is consistent with the framework adopted by Czuba et al. (2017) and Czuba (2018) in their models of network bed material routing.

Model reaches have a fixed channel geometry, but bed elevation and grain size distribution can vary with time. The channel is rectangular, with a fixed bankfull width, depth, and slope, and a length of 100 m. The bed is divided into an active layer representing bed sediment accessible to the flow (Parker, 1991, 2008), and a subsurface layer.

Initial channel conditions are determined by field observations and computations of the inferred bankfull capacity of our sites to transport sediment. Field measurements of channel morphology determine the model's bankfull width, depth, and slope; the initial grain size distribution of the model's bed is specified by field measurements of the stream bed at our sites. We assume an initial equilibrium bed elevation and bed material grain size distribution, and compute the sediment supply required to maintain the current bed configuration using the calibrated Wilcock and Crowe (2003) bedload transport equation with the measured channel morphology and bed material grain size distribution as input parameters. We refer to this computed sediment supply as $Q_{bT\ bed}$.

For each numerical experiment, additional sediment is added to the inferred existing supply $Q_{bT\ bed}$. Based on our conceptual model and field observations, we infer that additional fluvial sediment supply would be similar to the material currently found in gravel bars at our study sites, so the additional sediment is constrained to have the same grain size distribution measured from the bars at our field sites. The amount of additional sediment added represents the control variable for our numerical experiments; we denote the total sediment supply consisting of the background sediment feed $Q_{bT\ bed}$ plus the additional bar material as $Q_{bT\ supply}$.

We ran numerical experiments to represent 8 of our 12 sites. Sites 2, 9, 10, and 11 were not utilized due to absence of a suitable gravel bar; thus, the grain size distribution of the sediment supply could not be determined for these sites.

Numerical experiments were performed as follows. Using data from each site, sediment supply $Q_{bT\ supply}$ was varied over a wide range. For each value of $Q_{bT\ supply}$, the model was run for 20,000 days of bankfull flow. Successful runs achieved equilibrium, which was indicated when the grain size distribution of the bed material had reached a stable value that did not change significantly with time; see Bodek (2020) for details. The sediment flux through the channel at equilibrium is referred to as $Q_{bT\ eq}$. If equilibrium had been reached, the change bed elevation Δz_b was recorded as well as the mean grain diameter of the bed material, D_m.

Each experiment was interpreted using the criteria of Table 2. If the imposed sediment supply was sufficient for the bed to accumulate a developed subsurface and active layer, the experiment indicated a transition from a semi-alluvial to an alluvial channel. Alluvial conditions were reached when the bed aggraded to an elevation equal to or greater than the thickness of the active layer (L_a), which is based on the D_{90} of the bar material ($L_a = 2D_{90\ bed} = 0.2$ m). In this case, inerodible bedrock and colluvium was fully covered with fluvially-supplied sediment (Table 2). An alluvial outcome was also indicated when the mean grain size of the equilibrium bed matched the mean grain size of the bar material representing the sediment feed ($D_{m\ eq} = D_{m\ bar}$), indicating that the bed had become finer and was representative of the throughput load entering the reach (Table 2). By varying the flux of throughput load entering the reach ($Q_{bT\ supply}$), and the ratio $Q_{bT\ eq}/Q_{bT\ bed}$ as a result, we were able to determine the imposed flux of fluvial material needed to cause our sites to transform from their current semi-alluvial state to an alluvial channel whose bed material solely reflects sediment supplied by fluvial transport.

4.6.2 Numerical model equations

Changes in grain size distribution with time within the 100 m model domain are computed using equation (4) (Parker, 1991, 2008):

$$(1-\lambda_p)\left[L_a\frac{\partial F_{bi}}{\partial t}+(F_{bi}-F_{li})\frac{\partial L_a}{\partial x}\right]=-\frac{\partial q_{bi}}{\partial x} \tag{4}$$

where λ_p is the porosity of the bed (set equal to 0.3), L_a is the thickness of the active layer, F_{bi} is the fraction of grain size i on the bed, F_{li} is the fraction of grain size i at

Table 2. Possible Outcomes of the Numerical Model and their Interpretation

Variable	Outcome	Description
Bed elevation, z_b	$\Delta z_b = L_a$, $\Delta z_b > L_a$	Alluvial conditions reached; bed has aggraded to cover non-alluvial material
	$0 < \Delta z_b < L_a$	Semi-alluvial channel persists with some aggradation
	$\Delta z_b < 0$	Semi-alluvial channel persists with some erosion of bed material
Mean grain size, D_m	$D_{m\ eq} = D_{m\ bar}$, $D_{m\ eq} < D_{m\ bar}$	Alluvial conditions reached; bed GSD has fined and is representative of the throughput load entering the reach
	$D_{m\ eq} > D_{m\ bar}$	Semi-alluvial channel persists with some fining of the bed material

the interface between the active layer and the subsurface, q_{bi} is the volumetric bed material transport rate per unit width, t is time, and x is the downstream spatial coordinate. In solving equation (4), differential terms are represented by finite differences. For example, the term on the right is approximated as $-(q_{bi\ out}–q_{bi\ in})/dx$, where $q_{bi\ in}$ is the specified supply of grain size i from upstream, $q_{bi\ out}$ is the transport out of the study reach computed using the calibrated Wilcock and Crowe (2003) transport equation, and dx is 100 m. The interface grain size fraction, F_{li}, is based on a formulation by Hoey and Ferguson (1994). During erosion, subsurface material is incorporated into the active layer so F_{li} is equivalent to the fraction of grain size i in the subsurface. Alternately, during aggradation, F_{li} is a weighted mixture of sediments currently present in the active layer and bedload, such that $F_{li} = aF_{bi} + (1 - a)p_i$, where p_i is the fraction of grain size i in the bedload and a is an exchange parameter (set equal to 0.7).

Once fractional transport rates have been computed by solving equation (4), they are summed to determine the total bed material flux, $q_{b\ Total}$. Changes in bed elevation, z_b, over time are then determined by solving equation (5) (Parker, 1991, 2008):

$$\frac{\partial z_b}{\partial t} = -\frac{1}{(1-\lambda_p)}\frac{\partial q_{b\ Total}}{\partial x} \tag{5}$$

5 Results

5.1 Contemporary and ancestral longitudinal profile

The contemporary longitudinal profile of the White Clay Creek reveals two concave-upwards segments separated by a prominent knickpoint (Figure 1b). The knickpoint is located just downstream of Site 9, where the East Branch of the White Clay Creek flows through the bedrock-walled Laurel Gorge, slightly north of Landenberg, PA (Figure 1; Figure 5e).

The reconstructed long profile of an ancestral White Clay Creek obtained from equation (2) is illustrated in Figure 1b. The ancestral profile is constrained to pass through two points of the current profile with x coordinates of 1,000 m and 16,700 m, and elevations of 129 m and 74 m, respectively. The profile has a concavity parameter Q of 0.98. Near Newark, DE, the ancestral profile has a similar elevation as Old College Formation, which is exposed on both sides of the White Clay Creek valley (Figure 1b, 1c). The reconstructed ancestral profile is therefore consistent with Ramsey (2005), who hypothesized that the Old College Formation was deposited by a precursor of the White Clay

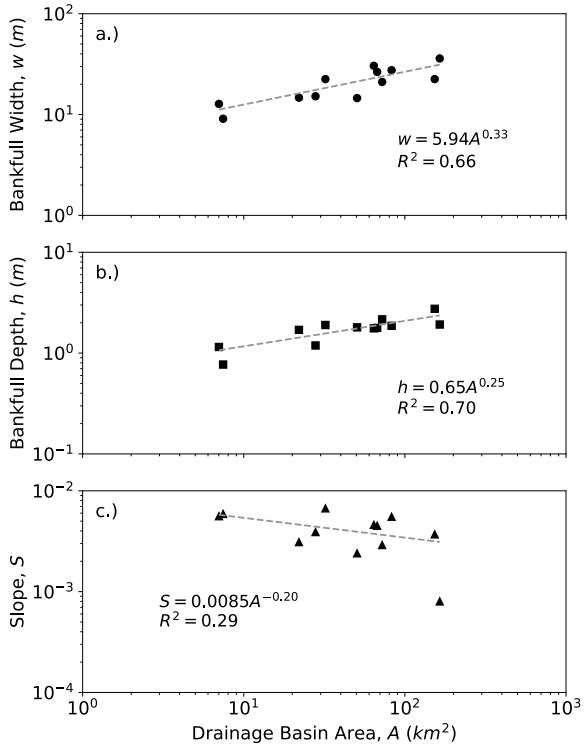

Figure 3. Relations between drainage basin area and (a) bankfull width, (b) depth, and (c) slope for the 12 study sites.

Creek during the middle Pleistocene. The White Clay Creek has incised approximately 50 m into the underlying bedrock since the middle Pleistocene, and a knickpoint has migrated upstream approximately 40 km. The morphology of the contemporary profile and the occurrence of Laurel Gorge at the knickpoint location suggests that knickpoint migration and the associated bedrock incision are continuing today.

5.2 Reach-scale morphology and landforms

The White Clay Creek is generally single-threaded and sinuous (sinuosity < 1.5), although 2 of the 12 sites have sinuosities in excess of 1.5 and could be considered meandering (Table 1). Five of the 12 sites display side channels or well-developed mid-channel bars. Bedrock and colluvium confine at least one bank at 9 of the 12 sites; confinement along both banks is rare, only occurring along short sections of Site 6 (in Laurel Gorge) and Site 14. Typically both bedrock and colluvium are exposed along banks, with bedrock underlying colluvium (although colluvium alone can be found in some banks). At locations where bedrock is exposed in channel banks, it is also typically exposed along the channel's bed. Eroding banks are pervasive, with bank retreat rates ranging from 2.6–32.1 cm/yr (Table 3). The 12 study sites have bankfull widths of 9.9–36.03 m, bankfull depths of 0.77–2.75 m, and slopes from 0.0008–0.0067 (Table 3). Width and depth are well-correlated with drainage basin area, while slope is not (Figure 3).

Median grain size of bed material ranges from 18.7–90.0 mm across the study sites, with half of the sites displaying median bed grain sizes in the pebble size range and half in the cobble size range (Table 3). The sand fraction of the bed material ranges from 0.09 to 0.28. Bankfull Shields stresses based on the median grain size of the bed material range

Table 3. Reach-scale Morphology and Sediment Transport Processes at the Study Sites

Site no.	Bankfull width	Bankfull depth	Slope	Median grain size		Fraction sand		τ_{*bf}	$\frac{\tau_{*bf}}{\tau_{*rm}}$	Lateral bank retreat rate
				$D_{50\ bed}$[a]	$D_{50\ bar}$[a]	$F_{s\ bed}$	$F_{s\ bar}$			
	[m]	[m]	[–]	[mm]	[mm]	[–]	[–]	[–]	[–]	[cm/yr]
1	22.47	2.75	0.0037	67.6	30.1	0.19	0.11	0.091	1.629	6.2
2	36.03	1.92	0.0008	40.2	NA[b]	0.13	0.55	0.023	0.414	32.1
3	15.19	1.19	0.0039	55.5	34.0	0.26	0.11	0.051	0.905	20.1
4	27.55	1.87	0.0055	57.9	23.9	0.13	0.08	0.108	1.922	5.8
5	21.06	2.16	0.0029	83.2	33.7	0.07	0.12	0.046	0.815	13.0
6	26.49	1.78	0.0045	79.5	27.7	0.11	0.09	0.061	1.090	4.9
8	14.71	1.70	0.0031	46.5	15.2	0.18	0.16	0.069	1.227	19.0
9	14.57	1.80	0.0024	28.4	ND[c]	0.28	ND	0.092	1.646	9.8
10	9.90	0.77	0.0059	18.7	ND	0.19	ND	0.147	2.629	12.4
11	12.75	1.15	0.0056	34.2	ND	0.14	ND	0.114	2.038	2.6
12	30.43	1.76	0.0046	81.4	30.9	0.10	0.10	0.060	1.076	9.1
14	22.45	1.90	0.0067	90.0	34.5	0.07	0.09	0.086	1.531	12.1

[a]Sand-sized sediment ($< 2mm$) was excluded from the grain size distribution when determining median grain size. This is because sand-sized sediment is expected to be transported in suspension during bankfull flows. [b]NA—not applicable. [c]ND—no data: some study sites lacked a well-developed gravel bar.

from 0.02 to 0.15 (Table 3). Dividing these values by the threshold Shields stress of 0.056 estimated from our tracer data (presented in Section 5.6) yields ratios between 0.41–2.63. These data fall within the range expected for alluvial, near-threshold, gravel-bed rivers (Figure 4).

The geomorphic setting and characteristic landforms of the White Clay Creek are further clarified by the geomorphic map of Site 4 (Figure 5a), which depicts a gently curving channel with well-developed pools, riffles, and runs—typical features of alluvial rivers found at all of our sites (Figure 5c). Boulders are scattered across the bed, some exceeding 1 m in diameter (Figure 5a, 5d). Bedrock and colluvium are occasionally exposed along the streambed or banks (Figure 5e); eroding colluvial banks are often mantled with angular boulders (Figure 5f, 5g), suggesting a local source for at least some of the boulders found on the channel bed. At Site 4 and two other sites (Table 1), a short section of the channel is confined by a 19^{th} century railroad grade (Figure 5a). Four bars at Site 4 have developed along the inside banks of bends, with laterally accreted floodplains developing near two of these bars. The outsides of bends at Site 4 are actively eroding cut-banks (Figure 5a). Similar features are found at all of our study sites (Figure 5c). At Site 4, several side channels are accessed during high flows (Figure 5a).

Figure 5b illustrates landforms at Site 1 that are typical of laterally migrating channels at our sites. Here the right bank is eroding at a slow rate of 0.06 m/yr, which is balanced on the left bank by lateral accretion of a low, sandy floodplain deposit inset beside a steep former bank; this bank was previously carved into valley fill deposits consisting of mud and sandy mud. A sandy point bar has developed on the left side of the channel immediately adjacent to the laterally accreted floodplain. The eroding right bank of the channel is higher than deposits of the left bank; however, analysis of flooding frequency at the USGS gaging station near Strickersville (located just downstream of the

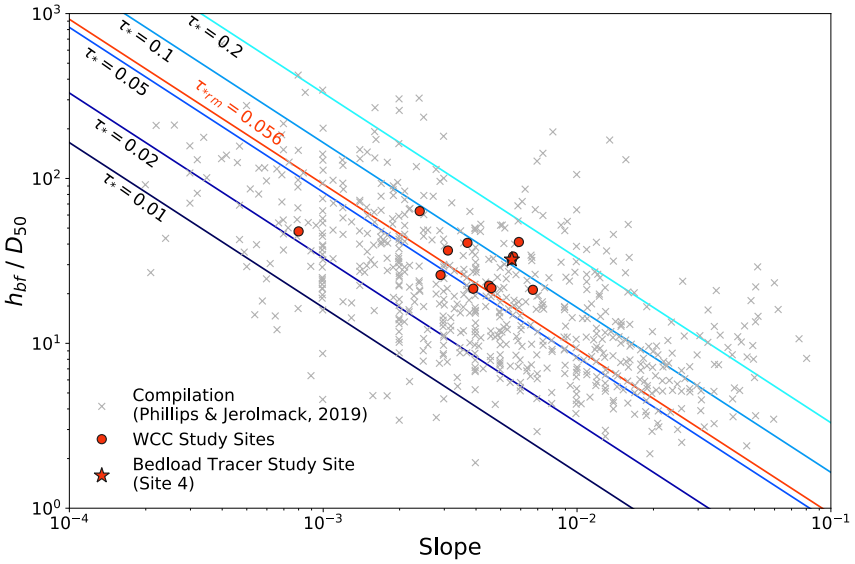

Figure 4. Bankfull relative submergence and slope for the White Clay Creek study sites and a compilation of data from alluvial, near-threshold, gravel-bed rivers from Phillips and Jerolmack (2019). Diagonal lines indicate values of constant Shields stress. The threshold Shields stress for incipient motion determined from bedload tracer studies at Site 4 of the White Clay Creek is indicated in red.

cross-section) using PEAKFQ software (Flynn et al., 2006) indicates that this surface is flooded frequently, with overbank flow occurring on average every 2.4 years.

The lithology and chronology of deposits in the eroding right bank of the cross-section in Figure 4b are also typical of our study sites. Cohesive sand and mud extend all the way to the base of the bank, indicating that bank erosion processes are decoupled from mobility of the gravel streambed, as noted by Pizzuto and Meckelnburg (1989) at the nearby Brandywine Creek. At the base of the bank, a spatially discontinuous, decimeter-thick layer of mud and sand with root and plant fragments is exposed. Radiocarbon dating of this layer yields ages of 1553–1699 (sample ID Beta-484923) and 580–652 (sample ID Beta-484924) calendar years BP (Pizzuto, Skalak, et al., 2020). A massive mud and sandy mud layer approximately 1 m thick overlies the organic-rich layer. A decimeter-thick dark grey to black horizon is exposed near the top of this unit; this dark layer has been described in valley fill deposits throughout the mid-Atlantic region, and is generally interpreted as a buried A horizon that represents the surface of the White Clay Creek's valley bottom at the time of European settlement (Happ et al., 1940; Jacobson & Coleman, 1986; Walter & Merritts, 2008). The uppermost unit consists of massive fine-medium grained sand and muddy sand. Dating of this deposit using ^{210}Pb, ^{137}Cs, and dendrochronology (Pipala et al., 2019; Pizzuto, Aalto, et al., 2020) demonstrates that these deposits are currently vertically accreting by active overbank deposition at rates approaching 1 cm/yr.

5.3 Contrasting grain size distributions of bed and bars

Grain size data indicate that bed and bar sediments of the White Clay Creek differ considerably (Figure 6). Bed material typically exhibits a modal grain size in the cobble range, with a significant proportion of boulders and abundant sand. Bars have a modal grain size in the pebble range, less sand than the bed, and no boulders (Figure 6a). Be-

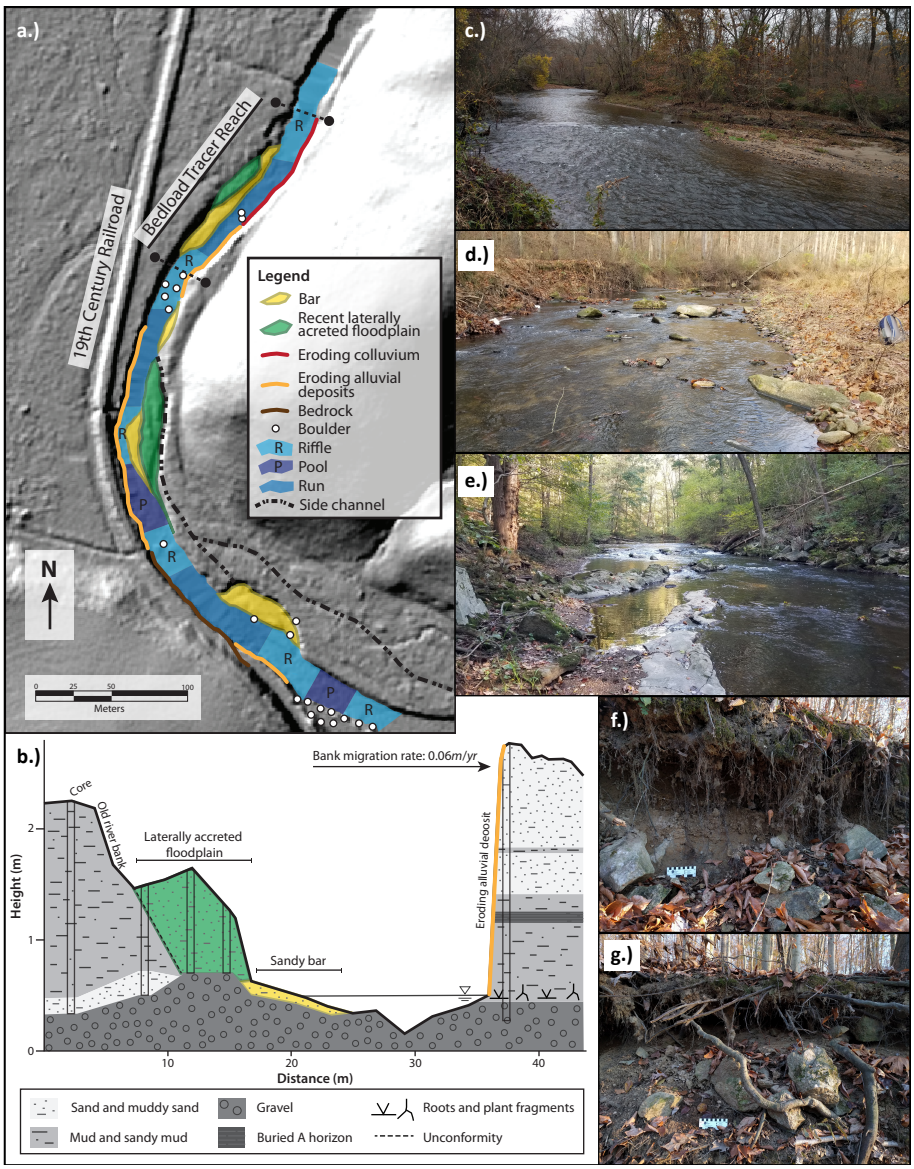

Figure 5. Representative geomorphic map, cross-section, and photographs illustrating characteristic features of the White Clay Creek study sites. (a) Geomorphic map of Site 4, which encompasses the bedload tracer study reach; (b) Cross-section at Site 1 showing typical stratigraphic relationships between landforms and a fully cohesive eroding bank. Photographs of the White Clay Creek show: (c) pools, riffles, and alternate bars just downstream of Site 2; (d) angular colluvial boulders on the streambed at Site 12—the left bank is actively eroding, while the right bank is a laterally accreting floodplain deposit; (e) exposed bedrock in the channel and steep valley walls of Laurel Gorge just downstream of Site 6; (f, g) hillslope supplying angular colluvial boulders on the left bank (facing downstream) of the White Clay Creek at Site 4.

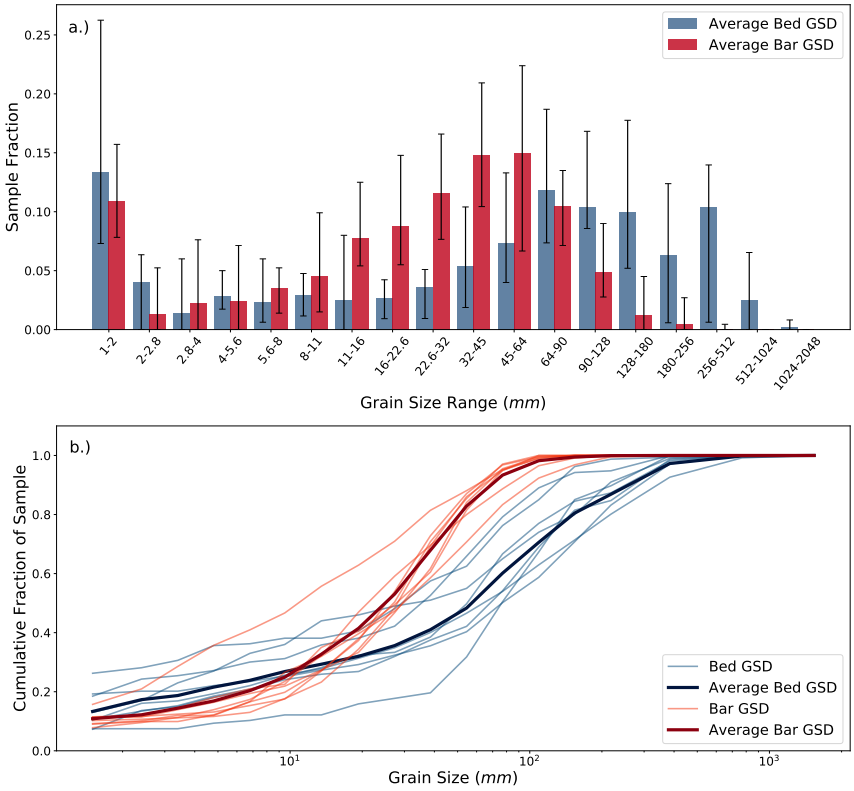

Figure 6. Grain size distributions for sediment in the White Clay Creek watershed: (a) average grain size distribution for bed and bar material, where error bars indicate the highest and lowest fraction of each grain size observed across the study sites; (b) cumulative grain size distribution for bed and bar material at 8 sites. Average bed and bar cumulative grain size distributions are also displayed. Average grain size distributions are based on pebble counts at Sites 1, 3, 4, 5, 6, 8, 12, and 14; these site parameters were used as initial model conditions.

cause bars are, by necessity, composed of readily transported material, the grain size distribution of the bars likely reflects sediments frequently mobilized as bedload by the White Clay Creek. We also hypothesize that the boulders found on the streambed (but absent from bars) likely represent sediments that are not commonly mobilized by frequent (i.e., bankfull) flows.

5.4 Bedload tracer particles

Four flows occurred during the active monitoring of tracer particles with stages that equaled or exceeded 1.86 m. The stage of 1.86 m is 2/3 of the *action stage* (referred to as *bankfull* hereafter) of 2.74 m defined by the USGS at the Strickersville gaging station. Three flows reached 2/3 of the bankfull stage (documented by surveys on 2 July 2019, 25 July 2019, and 5 November 2019), while the fourth event reached 92% of the bankfull stage (documented by a survey on 28 January 2020). Additional details are provided by Bodek (2020).

Based on cumulative results from the nine surveys, smaller grains tend to be more mobile than larger grains. Tagged clasts in the 11–45 mm size range were observed to have moved the most during the study period (Figure 7). Mobility decreases as clasts

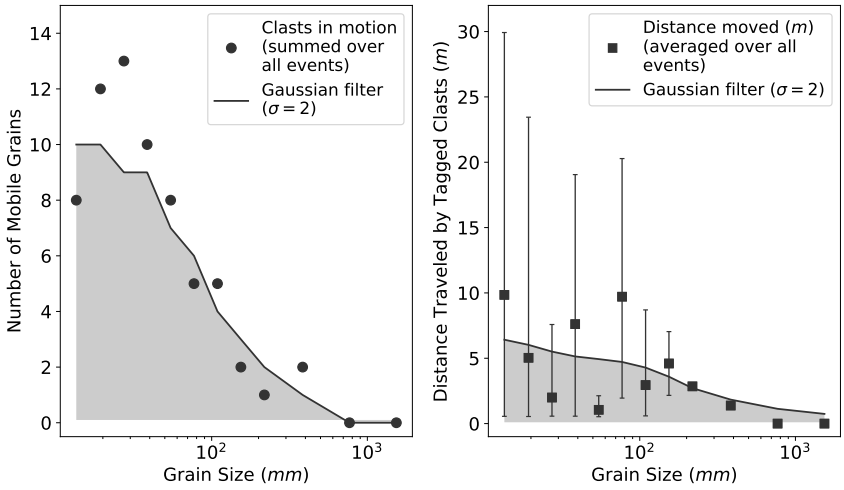

Figure 7. Mobility of each grain size category based on cumulative results from nine surveys: (a) number of clasts in motion summed over all nine events; (b) average distance traveled by tagged clasts per event. The error bars indicate individual events with the shortest and longest distance traveled. Both the number of tracer particles in motion and average distance traveled by tagged particles increases for smaller clasts.

become larger, with limited motion above 180 mm and no motion observed above 512 mm.

Data from events on 27 October 2019 and 25 January 2020 are used to calibrate the Wilcock and Crowe (2003) bedload transport equation. During the first event, the stage at the Strickersville gage height reached 1.86 m. The subsequent survey of bedload tracer particle locations indicated that 84.6% of the relocated tagged clasts were immobile (with a 93% recovery rate). Only smaller clasts (<80 mm) were transported by this event. During the second event, the Strickersville gage reached 2.52 m (92% of bankfull stage). This event mobilized 59.5% of the located tracers (with a 66% recovery rate). The largest mobile clast was 450 mm.

On 4 August 2020, 7 months after active monitoring of the tracer particles had ended, rainfall from Tropical Storm Isaias resulted in a peak stage of 3.99 m at the White Clay Creek gaging station near Strickersville. This event, estimated as a 50-yr flood (Gerald Kauffman, personal communication) at the White Clay Creek near Newark (USGS gaging station #01479000), was followed 3 days later by a peak stage of 3.47 m at the Strickersville gage as a result of unusually intense thunderstorms.

Tracer particles were resurveyed on 14 August 2020. Because multiple large events had occurred between surveys (including a near-bankfull event on 13 April 2020), only qualitative results could be obtained. Only 13 of the 56 tagged particles were found; these included nine boulders (all tagged boulders were found), three cobbles, and one pebble. Of these, four boulders with diameters from 340 mm to 800 mm moved a median distance of 1.5 m; one 450 mm boulder moved 39.4 m. The remaining boulders, with diameters from 420–1,440 mm, did not move. One cobble moved 28.9 m, while the other two cobbles were immobile. The 60 mm diameter pebble did not move. These data demonstrate that rare, extreme events will move some boulders short distances, while others remain immobile during even these exceptional discharges.

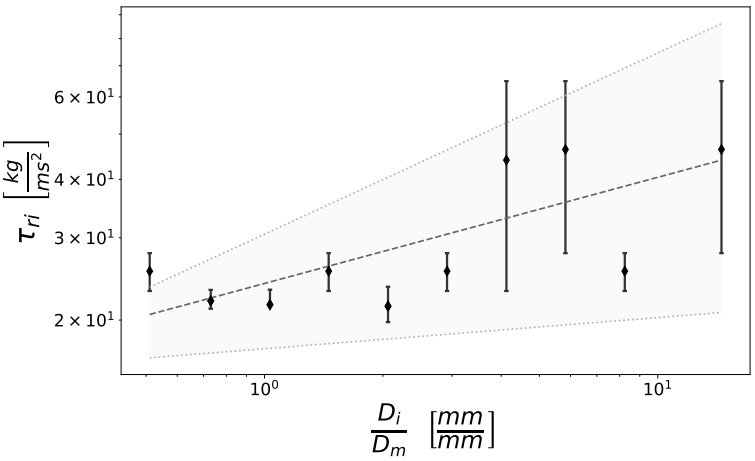

Figure 8. Reference shear stress is related to dimensionless grain size by a power function, where grain size is normalized by the mean grain size. Error bars indicate the range of reference shear stresses possible for each grain size based on bedload tracer data. The light gray lines bounding the trend line indicate a 5% and 95% confidence interval.

5.5 Bedload transport model calibration

To calibrate the Wilcock and Crowe (2003) transport equation, it is necessary to determine the reference shear stress of each grain size category. By plotting the reference shear stress of each grain size against normalized grain size (Figure 8), the reference shear stress for the mean grain size (τ_{rm}) and hiding function exponent (b) can be determined through linear regression:

$$\tau_{ri} = 23.95 \left(\frac{D_i}{D_m} \right)^{0.23} \tag{6}$$

where the coefficient indicates the reference shear stress of the mean grain size ($\tau_{rm} = 23.95$ kg/ms^2) and the exponent ($a = 0.23$) is related to the hiding function exponent by $b = a - 1$. Including the 95% confidence interval yields $\tau_{rm} = 23.95 \pm 6.58$ kg/ms^2 and $a = 0.23 \pm 0.16$.

The dimensionless reference shear stress for the mean grain size is $\tau_{*rm} = 0.056 \pm 0.015$. The hiding function exponentis $b = 0.77 \pm 0.16$. This yields the relationship between reference Shield's stress and normalized grain size:

$$\tau_{*ri} = 0.056 \left(\frac{D_i}{D_m} \right)^{-0.77} \tag{7}$$

5.6 Bed and bar sediment mobility at bankfull stage

The calibrated Wilcock and Crowe (2003) equation indicates that the largest clast on the bed at Site 4 that is expected to be mobile at bankfull stage is 187.0 mm, while the largest mobile clast on the bar is 198.4 mm. The largest mobile grain size differs for the Site 4 bed and bar material due to the hiding function. Thus, 85.7% of the bed material should be mobile at bankfull stage, while almost 100% of the bar material should be mobile under the same conditions (Table 4). Within the White Clay Creek Watershed, 92–100% of the bar material is expected to be mobile at bankfull stage, while only 27–92% of bed material is mobile.

Bodek (2020) supplements the estimates of bed mobility presented here based on the Wilcock and Crowe (2003) equation with additional bed mobility estimates based on the Shields diagram and threshold mobility values reported by Buffington and Montgomery (1997). While these analyses are not included here, the two methods generally provide similar results.

5.7 Sensitivity to sediment supply

Equilibrium bed elevations increase with increasing sediment supply (Figure 9a), while grain size of the equilibrium bed decreases with increased supply of bar sediment to the channel (Figure 9b). Study reaches positioned toward the right of Figure 9 (i.e., higher sediment supply ratio) are considered insensitive and require greater inputs of fluvially transported material before significant changes in bed elevation or mean grain size occur; those positioned toward the left (i.e., lower sediment supply ratio) are considered sensitive and readily aggrade or fine in response to increases in fluvially transported sediment flux.

Numerical model estimates of the ratio of $Q_{bT\ eq}/Q_{bT\ bed}$ needed to construct a fully-developed active layer range from 1.23 to 1.90 across the eight modeled study sites, suggesting that a roughly 20–90% or greater increase in bed material supply would be needed to transform the White Clay Creek into an alluvial channel (Figure 9a). The ratio of sediment fluxes that caused the mean grain size of the equilibrium bed to match that of the bar ranges from 1.3 to 2.92 across seven of the eight study sites (Figure 9b). Contradictory results were observed at Site 3, where the mean grain size of the bed material is finer than the bar material. With the exception of Site 3, an 11–200% increase in fluvially transported material would be needed to equalize the grain size distributions of the bed and bar sediments.

The two criteria used to determine if a modeled reach has developed alluvial characteristics generally agree across the different study sites (Figure 10). Thus, an insensitive site that requires a significant increase in the flux of throughput load to fine the bed also requires a similarly significant increase for the bed to aggrade. This trend does not apply to Site 3, where the mean grain size of the bed is finer than the mean grain size of the bar.

6 Discussion

6.1 Paradigms for classifying the White Clay Creek

6.1.1 The White Clay Creek as a bedrock river

Bedrock outcrops occur frequently along the White Clay Creek (Table 1), and a theoretical profile reflecting steady-state uplift and bedrock incision is consistent with the preserved middle Pleistocene longitudinal profile of the White Clay Creek and the elevation of the coeval alluvial fan sediments deposited by an ancestral White Clay Creek (Figure 1b, 1c). The present longitudinal profile indicates incision of approximately 50 m through the underlying bedrock since the middle Pleistocene, and the knickpoint at Laurel Gorge suggests that incision and knickpoint migration are ongoing. Reach-average slope is poorly correlated with drainage basin area (Figure 3c), providing further evidence that the longitudinal profile of the White Clay Creek continues to evolve.

These observations provide compelling evidence that the longitudinal profile of the White Clay Creek is controlled by bedrock erosion. According to several classification schemes (Meshkova et al., 2012; Turowski et al., 2008; Turowski, 2012) the White Clay Creek should be considered a bedrock river.

Table 4. Competence of WCC Study Sites Based on the Calibrated Wilcock and Crowe (2003) Sediment Transport Model

Site no.	Median grain size		Largest mobile grain size		Range of Largest Mobile Grain Size		Percent mobile		Range of mobile material	
	$D_{m\ bed}$[a] [mm]	$D_{m\ bar}$[a] [mm]	$D_{mobile\ bed}$ [mm]	$D_{mobile\ bar}$ [mm]	$D_{mobile\ bed}$ [mm]	$D_{mobile\ bar}$ [mm]	Bed [%]	Bar [%]	Bed [%]	Bar [%]
1	34.5	22.2	156.2	151.1	132.6–255.5	135.1–153.2	84.6	100.0	80.9-89.8	100.0
2	26.8	2.3	15.6	26.6	13.0–17.9	19.3–27.2	27.1	100.0	24.4–29.6	100.0
3	18.4	22.7	73.0	69.7	54.4–101.7	54.2–88.7	73.8	91.8	62.5–83.0	83.7–97.0
4	26.4	21.8	187.0	198.4	138.1–338.6	140.0–352.9	85.7	99.7	77.9–96.8	98.3–100.0
5	65.5	21.3	73.6	103.1	73.4–73.9	76.2–148.2	47.6	98.2	47.4–47.9	94.5–99.9
6	44.9	21.9	107.8	142.2	101.0–141.5	104.4–201.6	68.4	99.9	65.3–78.0	99.1–100
8	22.2	11.3	76.5	100.6	68.0–106.9	71.2–162.7	78.9	98.0	73.8–88.4	93.4–100
9	11.1	ND[b]	75.0	ND	53.8–123.4	ND	91.0	ND	84.4–96.2	ND
10	14.3	ND	74.7	ND	54.3–108.5	ND	92.0	ND	85.0–96.6	ND
11	24.0	ND	103.2	ND	76.6–145.7	ND	92.0	ND	83.8–97.2	ND
12	47.0	23.7	107.9	136.7	101.6–140.3	104.7–151.1	62.6	100.0	60.9–68.8	99.3–100
14	50.7	26.0	202.1	246.0	152.6–316.5	157.4–433.0	80.1	99.6	70.4–91.5	97.0–100
Avg[c]	30.2	16.2	106.7	134.5	90.8–147.8	96.5–214.1	77.1	99.1	72.5–84.7	96.7–99.9
Avg[d]	37.9	20.7	122.3	147.1	103.9–153.7	106.0–240.7	73.5	99.3	68.9–80.4	97.8–99.9

Note. The largest mobile grain size is determined using the Wilcock and Crowe (2003) sediment transport equation that has been calibrated to conditions at the bedload tracer study site. The range of largest mobile grain sizes is based on the range of hiding function exponents ($b = 0.93$ and $b = 0.61$) determined by the 5% and 95% confidence interval of the bedload tracer mobility data.
[a]Sand-sized sediment ($< 2mm$) was included in the grain size distribution when determining geometric mean size. Mean grain size was used for sediment transport calculations by Wilcock and Crowe (2003). [b]ND—no data; some study sites lacked a well-developed gravel bar.
[c]Average for all 12 study sites. [d]Average for 8 study sites with well developed gravel bars present (Site 1, 2, 3, 4, 5, 6, 8, 12, 14)

manuscript submitted to *JGR: Earth Surface*

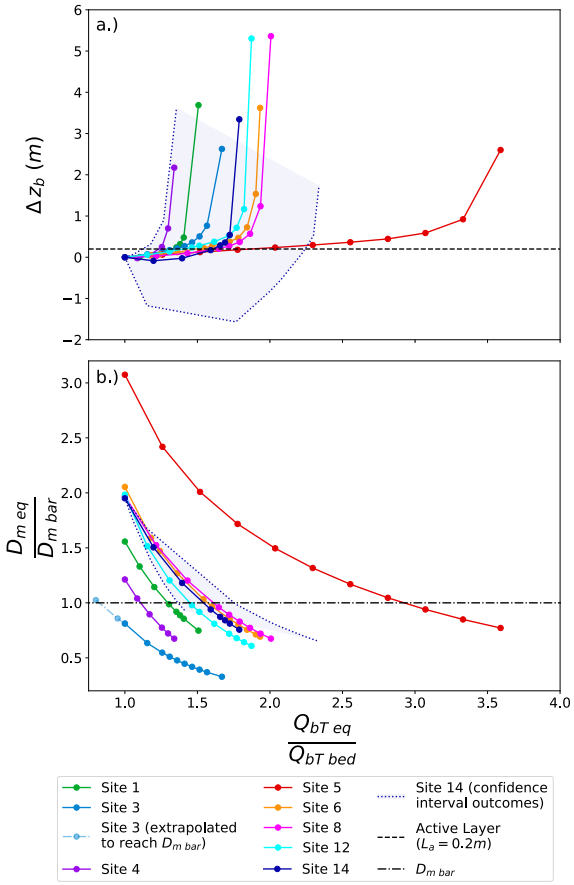

Figure 9. Changes in bed elevation and grain size for equilibrium conditions at the end of numerical simulations as functions of the sediment supply ratio $Q_{bt\ eq}/Q_{bt\ bed}$. The dotted lines and shaded area indicate the range of outcomes for Site 14 based on the 95% confidence intervals of τ_{*ri} and the hiding function exponent; these outcomes were calculated for all study sites. Two criteria were used to evaluate alluvial conditions: (a) changes in bed elevation, where the dashed line indicates transition from a semi-alluvial to an alluvial channel (i.e., when $\Delta z_b = L_a$); and (b) ratio of mean grain size of the simulated bed to measured bar mean grain size ($D_{m\ eq}/D_{m\ bar}$). The transition from a semi-alluvial channel to an alluvial channel occurs when this ratio equals one. Since Site 3 has a bar mean grain size that is coarser than the mean grain size of the bed, the reduction in sediment flux required to match the two mean grain sizes is extrapolated (pale blue line).

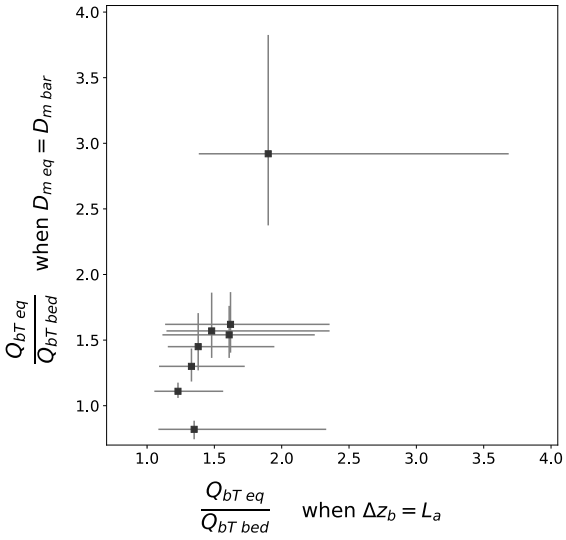

Figure 10. The ratio of sediment fluxes ($Q_{bT\ eq}/Q_{bT\ bed}$) at which the modeled reaches develop alluvial characteristics. The x-axis depicts the ratio of fluxes when the equilibrium bed elevation of a modeled reach has aggraded to cover the active layer. The y-axis indicates the ratio of fluxes when the mean grain size of the equilibrium bed matches the mean grain size of the bar material, which is representative of the throughput load. The error bars indicate the range of outcomes based on the 95% confidence intervals of τ_{*ri} and the hiding function exponent.

6.1.2 A quasi-equilibrium alluvial channel

The White Clay Creek displays prominent landforms characteristic of alluvial rivers, including pools and riffles, bars, and recently formed active floodplains. Well-developed hydraulic geometry equations for width and depth, and actively eroding banks all suggest that the channel cross-section is able to adjust to the current hydrologic regime. Following Wolman (1955), these observations support the idea that the White Clay Creek could at least partially be considered to represent a typical alluvial river, though we argue that this interpretation alone would be highly misleading.

6.1.3 The Anthropocene White Clay Creek

White Clay Creek has been highly influenced by human activities. *Legacy* sediments (Jacobson & Coleman, 1986; James, 2019; Pizzuto, 1987; Walter & Merritts, 2008), a result of watershed disturbances associated with 18^{th} and 19^{th} Century European colonization of the watershed, border the channel at all of our sites (e.g., Figure 5b). Sites of extant and former low-head mill dams can be found between many of our sites (Table 1). The White Clay Creek is locally confined by former railroad grades and other engineering structures (Table 1). Urban and suburban development have increasingly influenced watershed proceses in recent decades, though most development has occurred in the Delaware portion of the watershed downstream of our study sites (Kauffman & Belden, 2010).

These anthropogenic drivers have created well-documented impacts on stream channels in the region. Deposition of legacy sediments is associated with increased elevations of valley bottom surfaces, an effects that is enhanced upstream of mill dams. Urbanization has lead to widespread channel widening (Galster et al., 2008; Hammer, 1972; Pizzuto et al., 2000). Fluvial adjustments to many of these changes is likely ongoing.

Despite these important anthropogenic controls, the White Clay Creek displays landforms and deposits that are associated with "undisturbed" fluvial processes that should be evaluated from this perspective. These landforms include recently developed, laterally accreted floodplains, various types of bars, and pools and riffles. Although reaches of the channel with anthropogenic impacts can readily be identified where channels are bordered by thick mill pond sediments, the laminated muds that define these deposits pinch out upstream of former mill dams and are absent at our study sites (DeSonier et al., 2021; Huffman et al., 2021). Even floodplain surfaces underlain by historic legacy sediments continue to accrete vertically by ongoing overbank deposition (Pizzuto, Skalak, et al., 2020), though presenting specific evidence for this is beyond the scope of this manuscript. Our working hypothesis (to be evaluated in ongoing research) is that valley of the White Clay Creek is a mosaic of landforms and deposits, some derived directly from anthropogenic activity (e.g., mill pond deposits), some indirectly related to human actions, and others typical of undisturbed river systems.

6.1.4 A semi-alluvial, threshold, gravel-bed river

Bankfull Shields stresses and the range of bed sediment mobility at our sites are consistent with definitions of threshold gravel-bed rivers presented by Church (2006). Most of our sites have Shields stresses within the range that Church (2006) associates with cobble-bed, bedload dominated channels with low total transport in the partial transport regime; however, a few sites with Shields parameter values of approximately 0.1 or higher would likely fall into the category of sandy-gravel to cobble-gravel, bedload dominated streams. The Church (2006) description of the dynamic nature of the latter category is inconsistent with the low bank erosion rates of the White Clay Creek, but may be possible due to the influence of stabilizing bedrock exposures and coarse-grained colluvium.

The supply of coarse colluvium to the channel of the White Clay Creek is also consistent with the concept of the semi-alluvial river presented by Ashmore and Church (2000). Their inference that locally supplied coarse sediment imparts additional stability is also supported by the low bank erosion rates observed at our sites, despite some bankfull Shields values that Church (2006) would associate with his category of more active sandy-gravel to cobble-gravel streams. Although we cannot rigorously quantify the fraction of bed material supplied from colluvium, the fraction of cobbles and boulders may provide useful index. This index suggests that our sites represent a continuum of semi-alluvial, threshold, gravel-bed rivers ranging from *more* alluvial channels with predominately fluvially supplied sediment with relatively mobile beds to *more* semi-alluvial channels with an abundance of non-fluvially supplied sediment and relatively immobile beds (Figure 11).

6.1.5 The White Clay Creek as an ungraded channel

The concept of the graded stream (Mackin, 1948) suggests that rivers adjust their morphology to transport the supply of sediment, given the available discharge and other constraints. This concept is frequently cited and provides the basis for numerous quantitative models of reach-averaged equilibrium channel morphology (e.g., Chang, 1980; Millar, 2005; Parker, 1979). Furthermore, Wolman (1955) argued that hydraulic geometry relationships for the neighboring Brandywine Creek were a manifestation of this principle; this initially suggests that the White Clay Creek should also be considered a graded stream whose morphology is adjusted to transport the supply of fluvial sediment.

However, our modeling results indicate that the bed of the White Clay Creek is only partially mobile at bankfull stage, and more importantly, substantial increases in sediment supply can be accommodated without changing reach-averaged channel morphology. These conclusions are supported by (1) bedrock controls on the longitudinal profile and (2) the presence of locally sourced colluvium and weathered bedrock on the streambed, which indicate that bed elevation has not been solely adjusted by fluvial erosion and de-

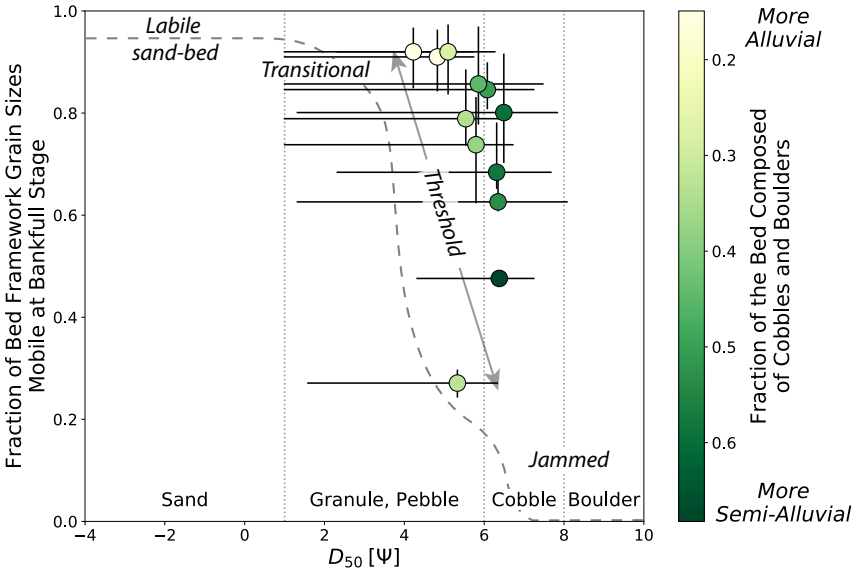

Figure 11. Data from the White Clay Creek and categories from Church (2006) based on median grain size and framework bed mobility. The line indicating bed mobility within each category is dashed to indicate uncertainty. The fraction of cobbles and boulders represents bed material sourced locally from colluvium and weathered bedrock. Vertical error bars indicate the fraction of mobile material based on the 95% confidence intervals of τ_{*ri} and the hiding function exponent; horizontal error bars indicate the D_{16} and D_{84} at each site. In many cases, the D_{16} is smaller than 2 mm and could not be accurately determined due to limitations in measuring fine grain sizes. Grain sizes are plotted using the Psi (Ψ) scale (Parker, 2008), defined by $ln(D_{50})/ln(2)$, with D_{50} in mm.

position. Apparently the morphology of the White Clay Creek is neither highly sensitive to, nor adjusted to, the supply of bed material.

6.2 Morphological controls on the White Clay Creek

6.2.1 Reconciling eroding banks with the threshold channel concept

As part of his explanation of threshold rivers, Parker (1978, 1979) suggested that gravel-bed rivers adjust their morphology such that gravel along the banks is at the threshold of motion at bankfull stage, while slightly higher shear stresses on the bed allow for transport of bed material supplied from upstream. According to this hypothesis, bankfull Shields stresses in gravel-bed rivers are limited to values only slightly in excess of those required to mobilize the bed, otherwise banks would become destabilized, resulting in additional channel widening. Rivers described by the Parker (1979) theory have bed and bank material consisting of unconsolidated, coarse gravel; in these channels, even grain sizes much coarser than the median pavement size are mobile at bankfull conditions. Parker (1979) described rivers in Alberta that exemplify these conditions, where the 2 year flood was capable of mobilizing grain sizes coarser than the D_{90}. Threshold channel theory (Parker, 1978, 1979) remains influential and has been supported by various compilation studies of rivers worldwide (e.g., Parker et al., 2007; Phillips & Jerolmack, 2016, 2019).

Despite bankfull Shields stresses that are generally consistent with the theory outlined by Parker (1978, 1979), other observations from the White Clay Creek are incompatible with this idea of stable, coarse-grained banks. Most importantly, banks are generally composed of cohesive sediment through to the bank toe as illustrated in Figure 5b and described by Pizzuto and Meckelnburg (1989), so gravel mobility is not coupled to bank stability; thus, morphology cannot be adjusted so that the (nonexistant) gravel at the bank toe is at the threshold of motion. Another contradiction is that 25 to 100% of banks at our study sites are actively eroding (Table 1) and would not be considered stable in the sense implied by Parker (1978, 1979).

6.2.2 Possible controls on width adjustment

The hydraulic geometry relation for width and, to a lesser extent, depth (Figure 3a, 3b), suggest that the White Clay Creek is able to maintain a quasi-equilibrium channel cross-section, which may or may not be slowly changing through time (e.g., Galster et al., 2008). If the mechanism proposed by Parker (1978, 1979) does not apply, then what processes could be responsible for maintaining stable channel width?

Banks of the White Clay Creek are highly variable; bedrock, colluvium, and engineering structures help stabilize the channel in many areas, while banks near former mill dams may be locally destabilized (Merritts et al., 2013). Although bank erosion is widespread, some banks are not eroding, while others are accumulating sediment. Given this diversity, is it difficult to apply a single paradigm that can represent reaches across the entire watershed.

At least two hypotheses merit further study. Where channels are migrating laterally (e.g., Site 1 in Figure 5b), the channel cross-section can be maintained by a balance between erosion and deposition as outlined by Allmendinger et al. (2005). Following this hypothesis, the width is governed by the ratio E/α, where bank erodibility (E) includes the effects of sediment type, vegetation, and erosional processes such as freeze-thaw. Meanwhile, the deposition parameter (α) reflects sediment trapping by vegetation, but might also be extended to included suspended sediment concentration and other variables. A second mechanism for maintaining channels with cohesive banks has been proposed by K. Dunne and Jerolmack (2018, 2020), who suggest that width adjustment should reflect the bank erosion threshold of the least erodible material composing the streambanks.

This concept could explain width adjustment in sections of the White Clay Creek with stable banks, if the appropriate erosion thresholds could be quantified and compared with the shear stresses imposed on the banks at relevant discharges.

A simple modification of the Allmendinger et al. (2005) approach might allow for the erosion threshold hypothesis proposed by K. Dunne and Jerolmack (2018, 2020) to closely approximate conditions at migrating sections. This idea can be achieved by replacing the erodibility constant of Allmendinger et al. (2005) with E', an erodiblity coefficient that is defined in excess of an erosion threshold, E_c, such that $E' = E - E_c$. For the very low bank erosion rates of the White Clay Creek (e.g., Table 3), E should only exceed E_c by a small amount. Thus, the erosion threshold should give a close approximation to both E and E', providing a means of correlating channel morphology with erodiblity thresholds as envisioned by K. Dunne and Jerolmack (2018, 2020), despite the presence of actively eroding banks.

7 Conclusions

The White Clay Creek is a semi-alluvial, threshold, gravel bed river whose longitudinal profile reflects bedrock incision. Its bed material represents a mixture of fluvially supplied sand and gravel, and cobbles and boulders eroded from local colluvial banks and weathered bedrock. The morphology of the White Clay Creek is not adjusted to transport the supply of bed material. Rather, the channel cross-section reflects erosion of cohesive bank sediments, strongly mediated by freeze-thaw processes and riparian vegetation, and possibly depositional processes as well. While the White Clay Creek has been strongly influenced by anthropogenic activity, the width and depth remain well-correlated with drainage basin area, indicating an ongoing adjustment to the watershed's prevailing hydrologic regime through erosion and deposition.

The morphology of the White Clay Creek reflects a variety of paradigms of fluvial geomorphology—from bedrock incision to alluvial erosion, from to sedimentation to processes associated with Anthropocene streams. Restoration and management of these channels should be guided by a broad, nuanced understanding of these diverse drivers rather than by any single conceptual model.

Acknowledgments

Financial support was provided by Delaware Watershed Research Fund Award #DWRF-16-109. Doug Jerolmack and Colin Phillips loaned instrumentation needed for tracking bedload tracer particles. Useful suggestions were offered by Melinda Daniels, Doug Jerolmack, and John Pitlick. We gratefully acknowledge thoughtful reviews of a previous version by JGR-ES Associate Editor Noah Finnegan and three perceptive anonymous reviewers. Supporting data can be found in Bodek (2020) and McCarthy (2018), which are available through figshare, a free and open repository. Bodek (2020) can be accessed using the included link (doi.org/10.6084/m9.figshare.14551290.v1) and McCarthy (2018) can be accessed using the provided link (https://doi.org/10.6084/m9.figshare.14561193.v1).

Attribution: SB performed the bedload transport monitoring and analysis, KEM and RAA surveyed the 12 study sites, KEM quantified bank erosion rates, and JEP supervised .

References

Allmendinger, N. E., Pizzuto, J. E., Potter Jr, N., Johnson, T. E., & Hession, W. C. (2005). The influence of riparian vegetation on stream width, eastern Pennsylvania, USA. *Geological Society of America Bulletin*, *117*(1–2), 229–243. doi:

10.1130/B25447.1

Andrews, E. (1984). Bed-material entrainment and hydraulic geometry of gravel-bed rivers in Colorado. *Geological Society of America Bulletin*, *95*(3), 371–378. doi: 10.1130/0016-7606(1984)95⟨371:BEAHGO⟩2.0.CO;2

Andrews, E. (1994). Marginal bed load transport in a gravel bed stream, Sagehen Creek, California. *Water Resources Research*, *30*(7), 2241–2250.

Andrews, E., & Parker, G. (1987). Formation of a coarse surface layer as the response to gravel mobility. In C. R. Thorne, J. C. Bathurst, & R. D. Hey (Eds.), *Sediment transport in gravel-bed rivers* (pp. 239–300). New York, NY: Wiley.

Ashmore, P., & Church, M. (2000). The impact of climate change on rivers and river processes in canada.

Bodek, S. (2020). *Is the White Clay Creek a threshold channel? Evaluating bed-mobility of a gravel-bed river, Pennsylvania, U.S.A.* (Master's thesis, University of Delaware, Newark, DE). doi: 10.6084/m9.figshare.14551290.v1

Buffington, J. M., & Montgomery, D. R. (1997). A systematic analysis of eight decades of incipient motion studies, with special reference to gravel-bedded rivers. *Water Resources Research*, *33*(8), 1993–2029. doi: 10.1029/96WR03190

Buffington, J. M., & Montgomery, D. R. (1999a). Effects of hydraulic roughness on surface textures of gravel-bed rivers. *Water Resources Research*, *35*(11), 3507–3521.

Buffington, J. M., & Montgomery, D. R. (1999b). Effects of sediment supply on surface textures of gravel-bed rivers. *Water Resources Research*, *35*(11), 3523–3530.

Chang, H. H. (1980). Geometry of gravel streams. *Journal of the Hydraulics Division*, *106*(9), 1443–1456.

Christopher, M., & Woodruff, K. (1982). *Thickness of Regolith in the Delaware Piedmont* (No. 19). Newark, DE: Delaware Geological Survey.

Church, M. (2006). Bed material transport and the morphology of alluvial river channels. *Annual Review of Earth and Planetary Science*, *34*, 325–354. doi: 10.1146/annurev.earth.33.092203.122721

Costa, J. E., & Cleaves, E. T. (1984). The piedmont landscape of Maryland: a new look at an old problem. *Earth Surface Processes and Landforms*, *9*(1), 59–74.

Czuba, J. (2018). A lagrangian framework for exploring complexities of mixed-size sediment transport in gravel-bedded river networks. *Geomorphology*, *321*, 146-152. doi: 10.1016/j.geomorph.2018.08.031

Czuba, J., Foufoula-Georgiou, E., Gran, K., Belmont, P., & Wilcock, P. (2017). Interplay between spatially explicit sediment sourcing, hierarchical river-network structure, and in-channel bed material sediment transport and storage dynamics. *Journal of Geophysical Research: Earth Surface*, *122*(5), 146-152. doi: 10.1002/2016JF003965

Dade, W. B., & Friend, P. F. (1998). Grain-size, sediment-transport regime, and channel slope in alluvial rivers. *Journal of Geology*, *106*(6), 661–676. doi: 10.1086/516052

Davies-Colley, R. J. (1997). Stream channels are narrower in pasture than in forest. *New Zealand Journal of Marine and Freshwater Research*, *31*(5), 599–608.

Del Vecchio, J., DiBiase, R. A., Denn, A. R., Bierman, P. R., Caffee, M., & Zimmerman, S. R. (2018). Record of coupled hillslope and channel response to Pleistocene erosion and deposition in a sandstone headwater valley, central Pennsylvania. *Geological Society of America Bulletin*, *130*(11-12), 1903–1917. doi: 10.1130/B31912.1

DeSonier, E., JE, P., & Huffman, M. (2021). Stratigraphy of valley fill deposits upstream of a small colonial-age mill dam, White Clay Creek, Pennsylvania. *Geological Society of America Abstracts with Programs*, *53*(1). doi: 10.1130/abs/

2021NE-361712

Dietrich, W. E., Kirchner, J. W., Ikeda, H., & Iseya, F. (1989). Sediment supply and the development of the coarse surface layer in gravel-bedded rivers. *Nature*, *340*(6230), 215–217.

Donovan, M., Miller, A., Baker, M., & Gellis, A. (2015). Sediment contributions from floodplains and legacy sediments to Piedmont streams of Baltimore County, Maryland. *Geomorphology*, *235*, 88–105. doi: 10.1016/j.geomorph.2015.01.025

Dunne, K., & Jerolmack, D. (2018). Evidence of, and a proposed explanation for, bimodal transport states in alluvial rivers. *Earth Surface Dynamics*, *6*(3). doi: 10.5194/esurf-6-583-2018

Dunne, K., & Jerolmack, D. (2020). What sets river width? *Science advances*, *6*(41), eabc1505. doi: 10.1126/sciadv.abc1505

Dunne, T., & Leopold, L. (1978). *Water in environmental planning.* New York, NY: Freeman.

Fischer, J. M., Riva-Murray, K., Hickman, R. E., Chichester, D. C., Brightbill, R. A., Romanok, K., & Bilger, M. D. (2004). *Water quality in the Delaware River Basin, Pennsylvania, New Jersey, New york, and Delaware, 1999-2001* (Vol. Circular 1227). Reston, VA: US Geological Survey.

Flynn, K. M., Kirby, W. H., & Hummel, P. R. (2006). *User's Manual for Program PeakFQ Annual Flood-Frequency Analysis Using Bulletin 17B Guidelines* (No. 4-B4). Washington, DC: U.S. Geological Survey. doi: 10.3133/tm4B4

Fryirs, K. A., Wheaton, J. M., & Brierley, G. J. (2016). An approach for measuring confinement and assessing the influence of valley setting on river forms and processes. *Earth Surface Processes and Landforms*, *41*(5), 701–710. doi: 10.1002/esp.3893

Galster, J. C., Pazzaglia, F. J., & Germanoski, D. (2008). Measuring the impact of urbanization on channel widths using historic aerial photographs and modern surveys. *Journal of the American Water Resources Association*, *44*(4), 948–960. doi: 10.111/j.1752-1688.2008.00193x

Hack, J. T. (1982). *Physiographic divisions and differential uplift in the Piedmont and Blue Ridge* (No. 1265). Reston, VA: U.S. Geological Survey.

Hammer, T. R. (1972). Stream channel enlargement due to urbanization. *Water Resources Research*, *8*(6), 1530–1540. doi: 10.1029/WR008i006p01530

Happ, S. C., Dobson, G. C., & Rittenhouse, G. (1940). *Some principles of accelerated stream and valley sedimentation* (No. 695). Washington, DC: U.S. Department of Agriculture.

Hassan, M. A., Brayshaw, D., Alila, Y., & Andrews, E. (2014). Effective discharge in small formerly glaciated mountain streams of British Columbia: Limitations and implications. *Water Resources Research*, *50*(5), 4440–4458. doi: 10.1002/2013WR014529

Hauer, C., & Pulg, U. (2018). The non-fluvial nature of Western Norwegian rivers and the implications for channel patterns and sediment composition. *Catena*, *171*, 83–98. doi: 10.1016/j.catena.2018.06.025

Hession, W., Pizzuto, J., Johnson, T., & Horwitz, R. (2003). Influence of bank vegetation on channel morphology in rural and urban watersheds. *Geology*, *31*(2), 147–150.

Hoey, T. B., & Ferguson, R. (1994). Numerical simulation of downstream fining by selective transport in gravel bed rivers: Model development and illustration. *Water Resources Research*, *30*(7), 2251–2260. doi: 10.1029/94WR00556

Huffman, M., Pizzuto, J., Symes, E., & DeSonier, E. (2021). Stratigraphy and depositional environments of the White Clay Creek, southeastern Pennsylvania. *Geological Society of America Abstracts with Programs*, *53*(1). doi: 10.1130/abs/2021NE-361835

Hupp, C. R., Noe, G. B., Schenk, E. R., & Benthem, A. J. (2013). Recent and

historic sediment dynamics along Difficult Run, a suburban Virginia Piedmont stream. *Geomorphology*, *180*, 156–169. doi: 10.1016/j.geomorph.2012.10.007

Inamdar, S., Johnson, E., Rowland, R., Warner, D., Walter, R., & Merritts, D. (2018). Freeze–thaw processes and intense rainfall: the one-two punch for high sediment and nutrient loads from mid-Atlantic watersheds. *Biogeochemistry*, *141*(3), 333–349. doi: 10.1007/s10533-017-0417-7

Jacobson, R. B., & Coleman, D. J. (1986). Stratigraphy and recent evolution of Maryland Piedmont flood plains. *American Journal of Science*, *286*(8), 617–637. doi: 10.2475/ajs.286.8.617

James, L. A. (2019). Impacts of pre-vs. postcolonial land use on floodplain sedimentation in temperate North America. *Geomorphology*, *331*, 59–77. doi: 10.1016/j.geomorph.2018.09.025

Kauffman, G. J., & Belden, A. C. (2010). Water quality trends (1970 to 2005) along Delaware streams in the Delaware and Chesapeake Bay watersheds, USA. *Water, air, and soil pollution*, *208*(1-4), 345–375. doi: 10.1007/s11270-009-0172-z

Kuhnle, R. A. (1993). Incipient motion of sand-gravel sediment mixtures. *Journal of Hydraulic Engineering*, *119*(12), 1400–1415. doi: 10.1061/(ASCE)0733-9429(1993)119:12(1400)

Li, R.-M., Stevens, M. A., & Simons, D. B. (1976). Morphology of cobble streams in small watersheds. *Journal of the Hydraulics Division, ASCE*, *102*(8), 1101–1117.

Lisle, T. E., Nelson, J. M., Pitlick, J., Madej, M. A., & Barkett, B. L. (2000). Variability of bed mobility in natural, gravel-bed channels and adjustments to sediment load at local and reach scales. *Water Resources Research*, *36*(12), 3743–3755. doi: 10.1029/2000WR900238

MacKenzie, L. G., & Eaton, B. C. (2017). Large grains matter: contrasting bed stability and morphodynamics during two nearly identical experiments. *Earth Surface Processes and Landforms*, *42*(8), 1287–1295. doi: 10.1002/esp.4122

MacKenzie, L. G., Eaton, B. C., & Church, M. (2018). Breaking from the average: Why large grains matter in gravel-bed streams. *Earth Surface Processes and Landforms*, *43*(15), 3190–3196. doi: 10.1002/esp.4465

Mackin, J. H. (1948). Concept of the graded river. *Geological Society of America Bulletin*, *59*(5), 463–512.

McCarthy, K. E. (2018). *Riverbank erosion rates in the White Clay Creek Watershed, PA* (Master's thesis, University of Delaware, Newark, DE). doi: 10.6084/m9.figshare.14561193.v1

Merritts, D., Walter, R., Rahnis, M., Cox, S., Hartranft, J., Scheid, C., ... Datin, K. (2013). The rise and fall of Mid-Atlantic streams: Millpond sedimentation, milldam breaching, channel incision, and stream bank erosion. In J. V. De Graff & J. E. Evans (Eds.), *The challenges of dam removal and river restoration* (21st ed., pp. 183–203). Boulder, CO: Geological Society of America. doi: 10.1130/2013.4121(14)

Merritts, D., Walter, R., Rahnis, M., Hartranft, J., Cox, S., Gellis, A., ... Winter, A. (2011). Anthropocene streams and base-level controls from historic dams in the unglaciated mid-Atlantic region, USA. *Philosophical Transactions of the Royal Society A: Mathematical, Physical and Engineering Sciences*, *369*(1938), 976–1009. doi: 10.1098/rsta.2010.0335

Meshkova, L. V., Carling, P. A., & Buffin-Bélanger, T. (2012). Nomenclature, complexity, semi-alluvial channels and sediment-flux-driven bedrock erosion. In M. Church, P. M. Biron, & A. G. Roy (Eds.), *Gravel-bed rivers: Processes, tools, environments* (pp. 424–431). Hoboken, NJ: Wiley Online Library. doi: 10.1002/9781119952497.ch31

Millar, R. G. (2005). Theoretical regime equations for mobile gravel-bed rivers with stable banks. *Geomorphology*, *64*(3-4), 207–220. doi: 10.1016/j.geomorph.2004

.07.001

Nelson, P. A., Venditti, J. G., Dietrich, W. E., Kirchner, J. W., Ikeda, H., Iseya, F., & Sklar, L. S. (2009). Response of bed surface patchiness to reductions in sediment supply. *Journal of Geophysical Research: Earth Surface*, *114*(F2). doi: 10.1029/2008JF001144

Noe, G. B., Cashman, M. J., Skalak, K., Gellis, A., Hopkins, K. G., Moyer, D., ... Hupp, C. (2020). Sediment dynamics and implications for management: State of the science from long-term research in the Chesapeake Bay watershed, USA. *Wiley Interdisciplinary Reviews: Water*, *7*(4), e1454. doi: doi.org/10.1002/wat2.1454

Parker, G. (1978). Self-formed straight rivers with equilibrium banks and mobile bed. part 2. the gravel river. *Journal of Fluid Mechanics*, *89*(1), 127–146. doi: 10.1017/S0022112078002505

Parker, G. (1979). Hydraulic geometry of active gravel rivers. *Journal of the Hydraulics Division, ASCE*, *105*(HY9), 1185–1201.

Parker, G. (1990). Surface-based bedload transport relation for gravel rivers. *Journal of hydraulic research*, *28*(4), 417–436. doi: 10.1080/00221689009499058

Parker, G. (1991). Selective sorting and abrasion of river gravel. i: Theory. *Journal of Hydraulic Engineering*, *117*(2), 131–147. doi: 10.1061/(ASCE)0733-9429(1991)117:2(131)

Parker, G. (2008). Transport of gravel and sediment mixtures. In M. Garcia (Ed.), *Sedimentation engineering: Processes, measurements, modeling, and practice* (pp. 165–251). Reston, VA: American Society of Civil Engineers.

Parker, G., & Klingeman, P. C. (1982). On why gravel rivers are paved. *Water Resources Research*, *18*(5), 1409–1423. doi: 10.1029/WR018i005p01409

Parker, G., Klingeman, P. C., & McLean, D. G. (1982). Bedload and size distribution in paved gravel-bed streams. *Journal of the Hydraulics Division, ASCE*, *108*(HY4), 544–571.

Parker, G., Wilcock, P. R., Paola, C., Dietrich, W. E., & Pitlick, J. (2007). Physical basis for quasi-universal relations describing bankfull hydraulic geometry of single-thread gravel bed rivers. *Journal of Geophysical Research: Earth Surface*, *112*(F4). doi: 10.1029/2006JF000549

Pavich, M., Brown, L., Valette-Silver, J. N., Klein, J., & Middleton, R. (1985). 10Be analysis of a Quaternary weathering profile in the Virginia Piedmont. *Geology*, *13*(1), 39–41.

Pazzaglia, F. J. (1993). Stratigraphy, petrography, and correlation of late Cenozoic middle Atlantic Coastal Plain deposits: Implications for late-stage passive-margin geologic evolution. *Geological Society of America Bulletin*, *105*(12), 1617–1634. doi: 10.1130/0016-7606(1993)105⟨1617:SPACOL⟩2.3.CO;2

Pfeiffer, A. M., Finnegan, N. J., & Willenbring, J. K. (2017). Sediment supply controls equilibrium channel geometry in gravel rivers. *Proceedings of the National Academy of Sciences*, *114*(13), 3346–3351. doi: 10.1073/pnas.1612907114

Phillips, C. B., & Jerolmack, D. J. (2014). Dynamics and mechanics of bedload-tracer particles. *Earth Surface Dynamics*, *2*(2), 513–530. doi: 10.5194/esurf-2-513-2014

Phillips, C. B., & Jerolmack, D. J. (2016). Self-organization of river channels as a critical filter on climate signals. *Science*, *352*(6286), 694–697. doi: 10.1126/science.aad3348

Phillips, C. B., & Jerolmack, D. J. (2019). Bankfull transport capacity and the threshold of motion in coarse-grained rivers. *Water Resources Research*, *55*(2), 11316—11330. doi: 10.1029/2019WR025455

Pico, T., Mitrovica, J. X., Perron, J. T., Ferrier, K. L., & Braun, J. (2019). Influence of glacial isostatic adjustment on river evolution along the US mid-Atlantic coast. *Earth and Planetary Science Letters*, *522*, 176–185. doi: 10.1016/j.epsl.2019.06.026

Pipala, J., Pizzuto, J., Stotts, S., Sherif, M., Sturchio, N., & LeBivic, R. (2019). Geochronology and stratigraphy of Holocene and recent sediments of the White Clay Creek Valley, southeastern PA. *Geological Society of America Abstracts with Programs*, *51*(1). doi: doi:10.1130/abs/2019NE-328060

Pizzuto, J. (1987). Sediment diffusion during overbank flows. *Sedimentology*, *34*(2), 301–317. doi: 10.1111/j.1365-3091.1987.tb00779.x

Pizzuto, J. (2009). An empirical model of event scale cohesive bank profile evolution. *Earth Surface Processes and Landforms*, *34*(9), 1234–1244. doi: 10.1002/esp.1808

Pizzuto, J., Aalto, R., Bodek, S., Karwan, D., Marquard, J., O'Neal, M., & Sturchio, N. (2020). Quaternary-present sediment transport and geomorphology of the White Clay Creek: Insights from geomorphic mapping and radionuclides. *Geological Society of America Abstracts with Programs*. doi: 10.1130/abs/2020SE-345266

Pizzuto, J., Hession, W., & McBride, M. (2000). Comparing gravel-bed rivers in paired urban and rural catchments of southeastern Pennsylvania. *Geology*, *28*(1), 79–82. doi: 10.1130/0091-7613(2000)028⟨0079:CGRIPU⟩2.0.CO;2

Pizzuto, J., & Meckelnburg, T. (1989). Evaluation of a linear bank erosion equation. *Water Resources Research*, *25*(5), 1005–1013. doi: 10.1029/WR025i005p01005

Pizzuto, J., O'Neal, M., & Stotts, S. (2010). On the retreat of forested, cohesive riverbanks. *Geomorphology*, *116*(3-4), 341–352. doi: 10.1016/j.geomorph.2009.11.008

Pizzuto, J., Skalak, K., Benthem, A., & Mahan, S. (2020). On the relative contribution of legacy sediments to some mid-Atlantic valley fill deposits. *Geological Society of America Abstracts with Programs*, *52*(6). doi: 10.1130/abs/2020AM-354756

Pizzuto, J., Skalak, K., Pearson, A., & Benthem, A. (2016). Active overbank deposition during the last century, South River, Virginia. *Geomorphology*, *257*, 164–178. doi: 10.1016/j.geomorph.2016.01.006

Plank, M. O., Schenck, W. S., & Srogi, L. (2000). *Bedrock geology of the Piedmont of Delaware and adjacent Pennsylvania* (No. 59). Newark, DE: Delaware Geological Survey.

Polvi, L. E. (2021). Morphodynamics of boulder-bed semi-alluvial streams in northern Fennoscandia: a flume experiment to determine sediment self-organization. *Water Resources Research*, *57*(3), e2020WR028859. doi: 10.1029/2020WR028859

Ramsey, K. W. (2005). *Geology of the Old College Formation Along the Fall Zone of Delaware* (No. 69). Newark, DE: Delaware Geological Survey.

Renner, G. T. (1927). The physiographic interpretation of the fall line. *Geographical Review*, *17*(2), 278–286.

Reusser, L. J., Bierman, P. R., Pavich, M. J., Zen, E.-a., Larsen, J., & Finkel, R. (2004). Rapid late Pleistocene incision of Atlantic passive-margin river gorges. *Science*, *305*(5683), 499–502. doi: 10.1126/science.1097780

Rhoades, E. L., O'Neal, M. A., & Pizzuto, J. E. (2009). Quantifying bank erosion on the South River from 1937 to 2005, and its importance in assessing Hg contamination. *Applied Geography*, *29*(1), 125–134. doi: 10.1016/j.apgeog.2008.08.005

Rice, S., & Church, M. (1996). Sampling surficial fluvial gravels; the precision of size distribution percentile sediments. *Journal of Sedimentary Research*, *66*(3), 654–665. doi: 10.2110/jsr.66.654

Schenck, W. S., Srogi, L., & Plank, M. O. (2000). *Bedrock Geologic Map of the Piedmont of Delaware and the Adjacent Pennsylvania* (No. 10). Newark, DE: Delaware Geological Survey.

Schenk, E. R., Hupp, C. R., Gellis, A., & Noe, G. (2013). Developing a new stream

metric for comparing stream function using a bank-floodplain sediment budget: a case study of three Piedmont streams. *Earth Surface Processes and Landforms*, *38*(8), 771–784. doi: 10.1002/esp.3314

Seal, R., & Paola, C. (1995). Observations of downstream fining on the North Fork Toutle River near Mount St. Helens, Washington. *Water Resources Research*, *31*(5), 1409–1419. doi: 10.1029/94WR02976

Segura, C., & Pitlick, J. (2015). Coupling fluvial-hydraulic models to predict gravel transport in spatially variable flows. *Journal of Geophysical Research: Earth Surface*, *120*(5), 834–855. doi: 10.1002/2014JF003302

Snyder, N. P., Castele, M. R., & Wright, J. R. (2009). Bedload entrainment in low-gradient paraglacial coastal rivers of Maine, USA: Implications for habitat restoration. *Geomorphology*, *103*(3), 430–446. doi: 10.1016/j.geomorph.2008.07.013

Stotts, S., O'Neal, M., Pizzuto, J., & Hupp, C. (2014). Exposed tree root analysis as a dendrogeomorphic approach to estimating bank retreat at the South River, Virginia. *Geomorphology*, *223*, 10–18. doi: 10.1016/j.geomorph.2014.06.012

Sweeney, B. W., Bott, T. L., Jackson, J. K., Kaplan, L. A., Newbold, J. D., Standley, L. J., ... Horwitz, R. J. (2004). Riparian deforestation, stream narrowing, and loss of stream ecosystem services. *Proceedings of the National Academy of Sciences*, *101*(39), 14132–14137. doi: 10.1073/pnas.0405895101

Trimble, S. W. (1997). Stream channel erosion and change resulting from riparian forests. *Geology*, *25*(5), 467–469.

Turowski, J. M. (2012). Semi-alluvial channels and sediment-flux-driven bedrock erosion. In M. Church, P. M. Biron, & A. G. Roy (Eds.), *Gravel-bed rivers: Processes, tools, environments* (pp. 399–418). Hoboken, NJ: Wiley Online Library. doi: 10.1002/9781119952497.ch29

Turowski, J. M., Hovius, N., Wilson, A., & Horng, M.-J. (2008). Hydraulic geometry, river sediment and the definition of bedrock channels. *Geomorphology*, *99*(1-4), 26–38. doi: 10.1016/j.geomorph.2007.10.001

Walter, R. C., & Merritts, D. J. (2008). Natural streams and the legacy of water-powered mills. *Science*, *319*(5861), 299–304. doi: 10.1126/science.1151716

Whipple, K. X., & Tucker, G. E. (1999). Dynamics of the stream-power river incision model: Implications for height limits of mountain ranges, landscape response timescales, and research needs. *Journal of Geophysical Research: Solid Earth*, *104*(B8), 17661–17674.

Wilcock, P. R. (1993). Critical shear stress of natural sediments. *Journal of Hydraulic Engineering*, *119*(4), 491–505. doi: 10.1061/(ASCE)0733-9429(1993)119:4(491)

Wilcock, P. R. (2001). Toward a practical method for estimating sediment-transport rates in gravel-bed rivers. *Earth Surface Processes and Landforms*, *26*(13), 1395–1408. doi: 10.1002/esp.301

Wilcock, P. R., & Crowe, J. C. (2003). A surface-based transport model for sand and gravel. *Hydraulic Engineering*, *129*(2), 120. doi: 10.1061/(ASCE)0733-9429(2003)129:2(120)

Wilcock, P. R., & McArdell, B. W. (1997). Partial transport of a sand/gravel sediment. *Water Resources Research*, *33*(1), 235–245.

Wolman, M. G. (1954). A method of sampling coarse river-bed material. *EOS, Transactions American Geophysical Union*, *35*(6), 951–956.

Wolman, M. G. (1955). *The natural channel of Brandywine Creek* (No. 271). Reston, VA: U.S. Geological Survey.

Wolman, M. G. (1959). Factors influencing erosion of a cohesive river bank. *American Journal of Science*, *257*(3), 204–216.